STAT [redacted]

TASK ORDER NO. 03(100,762)65-R

# ELECTROPHOTOGRAPHIC PROCESSING TECHNIQUES

SECOND INTERIM TECHNICAL REPORT



STAT [redacted]

STAT [redacted]

Issued: April 25, 1966

Electrophotographic Processing Techniques

STAT [redacted] Task Order No. 03(100,762)65-R

Errata Sheet for Second Interim Report

STAT [redacted] R-2957, Issued April 25, 1966)

1. Pages 32, 34, 35 - All references to film type SO 243 should be changed to film type 3404.

2. Page 34 - Delete on the fourth line from the bottom of the page:
"which has demonstrated printing resolution greater than 500 cycles per millimeter."

3. Page 63 - Add at top left of picture:
"Note: Sensing light is assumed as being 1.0 foot lamberts".

4. Page 76 - Change last line of second paragraph from the bottom of the page to read:
"$u(|x|) - u(|x| - x_o)$. The function $t_o(x)$ is Gaussian in nature."

STAT [redacted]

TASK ORDER NO. 03(100,762)65-R

# ELECTROPHOTOGRAPHIC PROCESSING TECHNIQUES

SECOND INTERIM TECHNICAL REPORT

STAT [redacted]

STAT [redacted]

Issued: April 25, 1966

## PREFACE

This is the second of a series of interim technical reports on a study of electrophotographic processing techniques. This twelve-month study comprises the investigation and development of photographic and electronic techniques for processing photographic images. This report covers the work performed by the [redacted] STAT
[redacted] STAT
ing the period from October 22, 1965 to February 22, 1966.

[redacted] STAT

TABLE OF CONTENTS

TABLE OF CONTENTS (Continued)

# LIST OF ILLUSTRATIONS

LIST OF ILLUSTRATIONS (Continued)

LIST OF ILLUSTRATIONS (Continued)

# SECTION I

# INTRODUCTION

## A. SUMMARY

The Electrophotographic Processing Techniques program covers the investigation, development, and evaluation of electrical-chemical and electronic techniques for processing photographic images to improve their perceptibility to human observers. This report describes the work done on this contract during the period from November 1965 to February 1966. It supplements a previous Interim Report of December 16, 1965 covering the period from July to October 1965.

The activities on the program have been divided into three major task groupings:

1. Electrical-Chemical Processing Techniques, which includes the classification of different types of transparencies, the use of chemical and optical techniques along with a modulated-light printing source for density manipulation to control acutance and granularity in processing transparencies, and the investigation of programmed sequences of these techniques and existing or possible future tools in processing transparencies of different types.
2. Electronic Processing Techniques, which includes the construction of breadboard electronic processors and experimentation with these processors to determine the usefulness and numerical requirements of various techniques to operate on high- and low-frequency information in photographic images and to determine the feasibility of practically implementing these techniques.
3. Technique Analysis, which includes the evaluation of both current and potential capabilities of the techniques investigated on the program, the development of a mathematical model of electronic processing systems, and the application of this model to current and contemplated systems.

Each of the task groupings are discussed separately in the sections that follow. For convenience, a brief summary of each of these sections is given below.

During the reporting period just completed, the electrical-chemical processing activity was concerned with processing both specially prepared combination target-scene transparencies and real imagery from film supplied by the customer. The target-scene combinations were degraded in three different ways - by

defocussing, by over-exposure and by simulating image motion The degraded pictures were compared with the undegraded original to determine the effect on densities in the transparencies and on image perceptibility. Utilizing these comparisons, photo-chemical techniques (generation of density mask overlays and manipulation of densities) were used to try to correct the degraded pictures (to obtain characteristics similar to the original). This correction phase was limited to the defocussed pictures, however, because of greater customer interest in other techniques and in real imagery processing, it was only carried far enough to show the trend of the correction.

The effect on real imagery processing was concentrated on selecting frames, choosing areas of interest for improvement in these frames, and performing image improvement experiments. Two very small areas (containing a resolution target and an aircraft) in one frame were selected for improvement. Phase-amplitude modulation techniques were applied using a phase-contrast microscope. Contrast improvements were obtained; additional imagery was perceptible in the improved picture.

Actual photo processing using the breadboard cathode-ray tube, modulated-light, and contact printer was not accomplished during this reporting period. Modifications were made to the printer to improve its operation and certain initial measurements and tests were made with it. Some additional corrections are now being made to this printer and it should be available for use shortly after the date of this report.

The Electronic Processing activity included the completion of the experiments with the low-resolution electronic processor, the analysis of experimental results, and the initiation of the assembly of the high-resolution processor. Experiments were made to determine the overall feasibility of a two-kinescope system for modulated-light processing and to examine effects on density manipulation and resolution. Problems of registration and positive or negative modulation control were specifically examined. In addition, several image-enhancement experiments, e.g., on edge effects, were conducted. All such experiments were examined with respect to design requirements for the high-resolution system. The low-resolution processor was disassembled prior to the writing of this report and the high-resolution system is in the process of being assembled.

The Techniques Analysis activity included an examination of the features of various modulated-light processing systems, the development of a general mathematical model of such systems, and the inital application of the model to help analyze the capabilities of the systems. Specifically, the model has been developed in terms of both the line-spread functions (LSF) and the modulation-transfer functions (MTF) of the systems components. Systems LSF's and MFT's have developed, and processing effects, such as edge gradients effects, were demonstrated using the model.

## B. PLANS FOR THE REMAINDER OF THE EPT PROGRAM

The remainder of the program will consist of a concentrated effort of experimentation and analysis for both the electrical-chemical and the electronic processing techniques. For the former, the initial work must include the testing and measurements of the capabilities of the modulated-light CRT printer. This will include, for combinations of different exposure and modulation levels, measurements of uniformity of illumination across the film, measurements of density-matching capability, evaluation of the effects of format and spot size changes, measurements of printing resolution, and calibration of the photocells used on the viewing screen. When this set of measurements is completed, the CRT printer will be used for the actual processing of pictures. A limited set of pictures with different types of imagery under different conditions will be selected and their characteristics described. Various combinations of controlled printing and developing will be tried to enhance different features in the pictures. Analyses will be made of the resultant pictures, using the different combinations of processing, and a program of suggested processing sequences will be suggested according to the types of features desired and the picture characteristics. Reprocessing according to these programs will be done on the same or similar pictures to determine the validity of the program sequences and to simulate what might be done in an integrated processor.

As time permits, there will be some further analysis on the applicability of optical processing techniques (such as phase and amplitude modulation) to larger, more complex image areas. Suggestions for further analysis will be made.

The remaining work on the study of electronic processing techniques involves the completion of the assembly, the testing, and the use of the high-resolution processor. The use of the processor will involve a series of experiments to check out the capabilities of the processor and then to determine the requirements for various existing or potential processing features. Experiments conducted for the low-resolution processor will be repeated first on the new processor and then additional experiments will be conducted. The features to be examined will include, time permitting, optimum modulation spot size, positive and negative masking, compensation for the sensing light, registration problems, comparison of isotropic and unidirectional scan, and other image-enhancement experiments. Recommendations will be made on the feasibility and desirability of incorporating new or modified features in an operational electronic processor.

The techniques analysis activities remaining on the program include first the completion of various checkout tests of the mathematical model. The results of both electronic and electrical-chemical processing will then be analyzed using the model to determine current capabilities and limitations inherent in the processes. Modifications and expansions will be made of the model to improve its

usefulness, if possible. As a result of this analysis, suggestions will be made for avenues of study or for specific techniques that should be considered for photograph processing.

# SECTION II

# ELECTRICAL-CHEMICAL PROCESSING TECHNIQUES

## A. GENERAL

The Electrical-Chemical Processing Techniques portion of the EPT Program is directed toward the development of photographic techniques that will contribute toward improved image qualification. Current emphasis is on the elevation of imagery from the subliminal levels to a prescribed recognition level. Image qualification is established by viewing positive transparencies on a specific light table (Richards). In this manner the degree of improvement in terms of information retrieval can be compared between the original and the corrected transparencies. The corrected copy will contain the same scale factor as defined by the original photographic frame.

To establish a suitable criterion for elevation of images located in the subliminal region, two approaches were considered. In the first approach, recognizable images were reduced, under controlled conditions, to a subliminal level. Several techniques were applied to elevate the images back to the original recognition level. In the second approach, using an operational scene and utilizing other techniques, subliminal images were elevated to recognition levels.

## B. PROCESSING EXPERIMENTS

### 1. Controlled Image Degradation and Correction

A relatively good quality aerial scene of the Libyan Desert, shown in Figure II-1, was selected for the image degradation and correction experiment. The basis for the selection was that the scale factor of 60,000 to 1 meant that there would be many micro-image elements, and that the scene contained only one type of subject; namely, sand dunes.

To determine the degree of degradation and correction, a density-resolution array target was used in the experiment. The array configuration and the density relationships are shown in Figure II-2. The manner in which the density-resolution array was combined with the aerial-scene film is shown in Figure II-3. Three individual types of degradation were selected: (1) defocus, (2) overexposure, and (3) image motion. For the defocus case, if the optimal focus is at a distance of $S'$, then the defocus distance increment becomes $+\Delta S'$. The total distance between the lens and the image plane then becomes $S' + \Delta S'$.

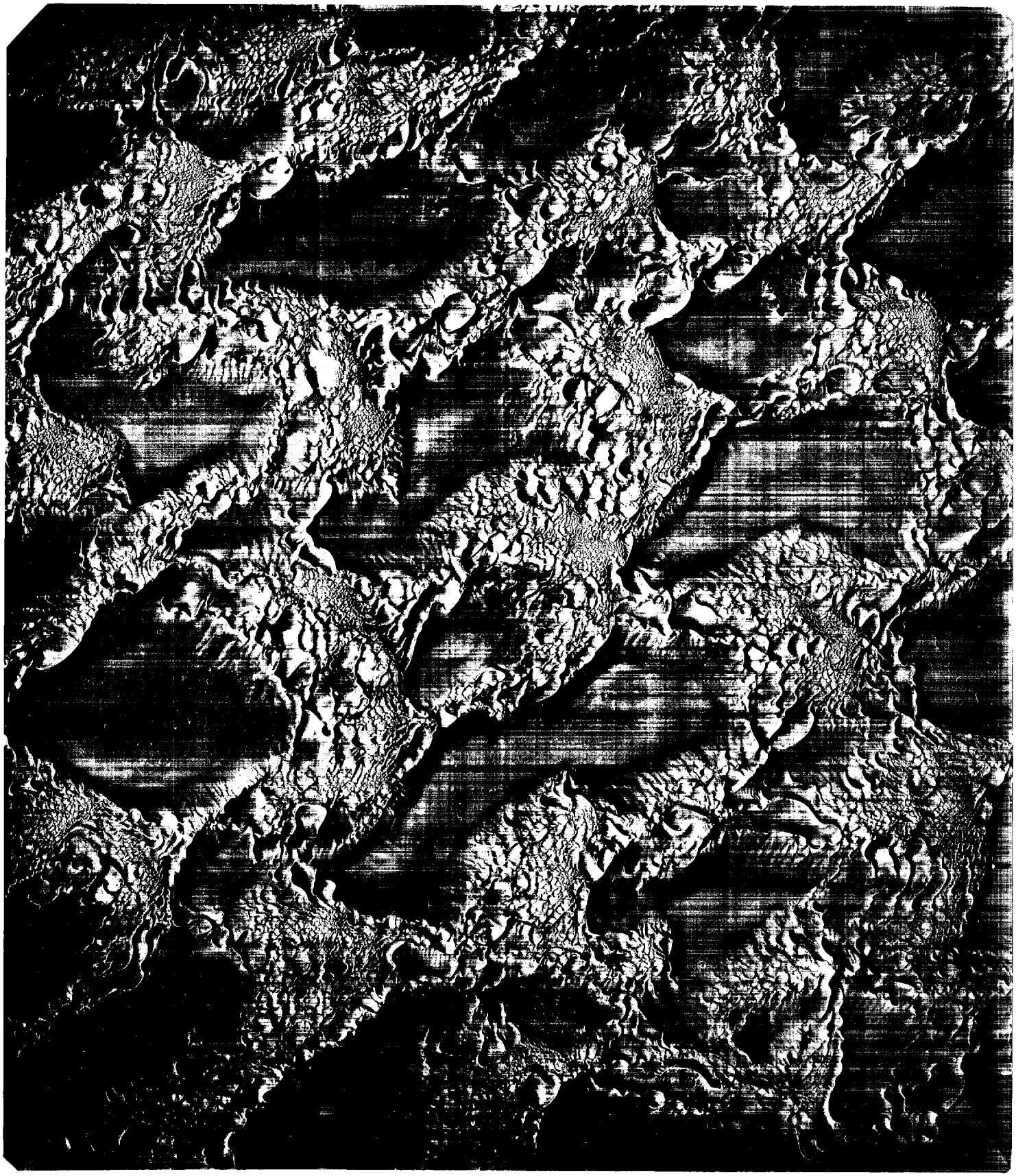

Figure II-1. Libyan Desert, Results of Image Degradation and Correction Experiment

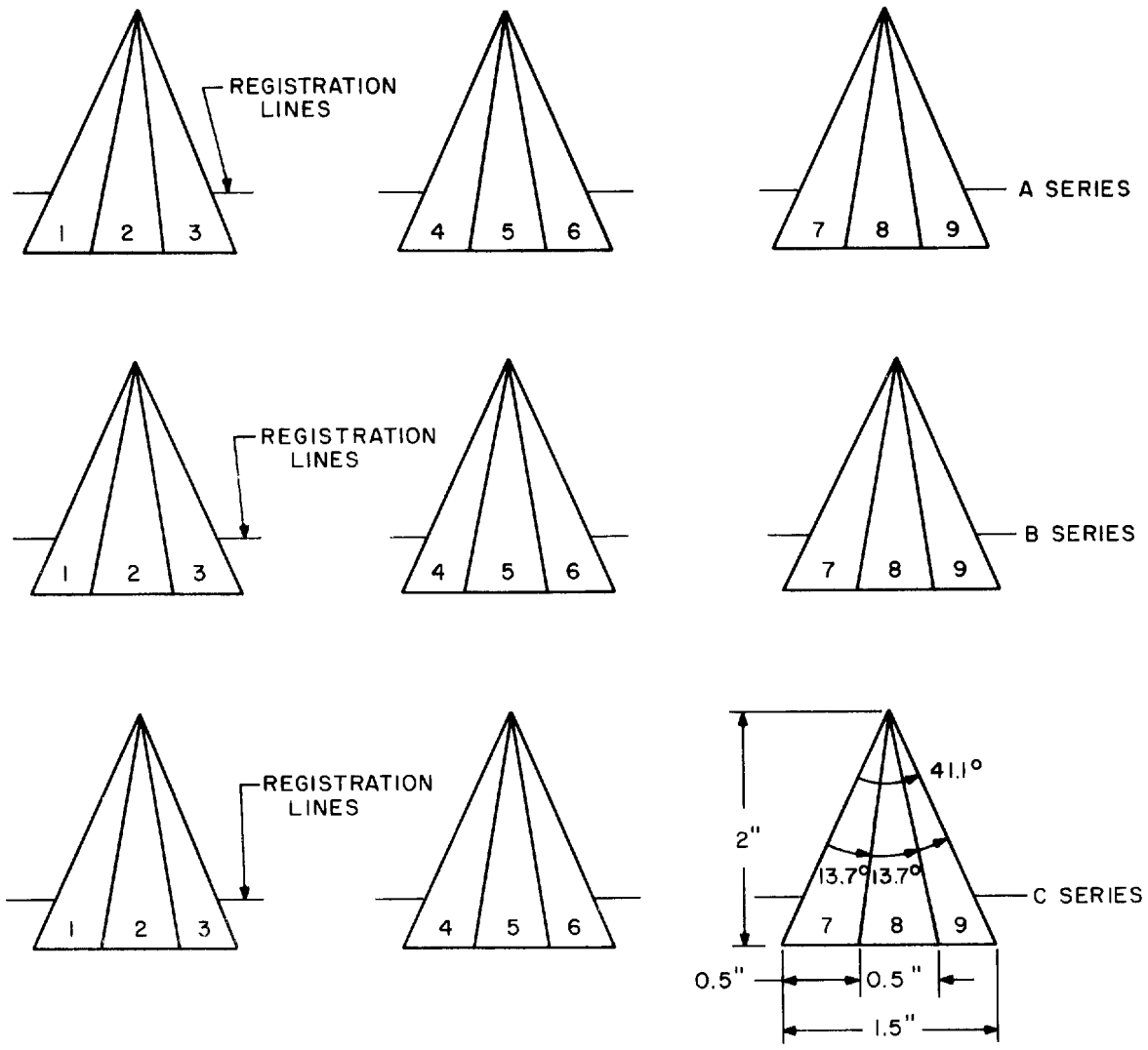


DENSITY TABLE

| | 1 | 2 | 3 | 4 | 5 | 6 | 7 | 8 | 9 |
|---|---|---|---|---|---|---|---|---|---|
| A | 1.90 | 1.30 | 1.04 | 0.91 | 0.79 | 0.57 | 0.45 | 0.31 | 0.12 |
| B | 0.12 | 0.59 | 1.0 | 1.32 | 0.79 | 1.30 | 0.32 | 0.90 | 1.90 |
| C | 0.12 | 0.33 | 0.49 | 0.59 | 0.79 | 0.90 | 1.0 | 1.27 | 1.90 |

Figure II-2. Resolution-Density Target Array with Density Table

The value for $\Delta S'$ was 2.5 millimeters. Overexposure time increments were 2× and 4×, respectively, that of the nominal exposure time. Image motion was in one direction at a constant rate of 0.4 millimeter per second during the nominal exposure time of 4 seconds. Exposure time and chemical processing were held constant in the preparation of the standard, defocused, overexposed, and image-motion specimens of the scene.

An outline of the procedures in the preparation of degraded image specimens and the subsequent correction cycle are shown in Figure II-4.

The procedure of preparing corrected images of defocus, overexposure, and image motion employs, at most, two techniques for each of the degraded negatives or transparencies: one is the overlay technique, and the second is the density-correction technique. The overlay technique was used primarily to correct image elements in the scene by suppressing additional unwanted densities that arise as a result of degradation. Where a single density in the original is degraded to a spectrum of densities, an overlay is used to reduce, as much as is possible, the number of additional densities by balancing the deviations through the addition of small incremental densities. The density-correction technique involves changing the gamma of exposure; densities that were shifted in the degradation are thereby corrected back to the original level. In the experiments, the density-correction technique was employed primarily for densities of the target in the test array. Density corrections were also made as a second step on the results of the use of the overlay technique.

a. Preparation of Samples

As previously indicated, the aerial photograph of the Libyan Desert, taken at a scale factor of 60,000 to 1, was selected for its many micro-image elements of the sand dunes as well as the micro-contrast ratio relationship of the picture elements in the scene. Since the negative had non-periodic picture elements, an array of triangles was introduced in the center of the scene. The process whereby test samples were prepared to include the triangles in the scene is described in the paragraphs that follow.

A target containing the triangle array was photographically reduced from 9-1/2 × 9 inches to 3-1/2 × 3-3/4 inches. The reduction was made on the HLC microcopy camera. Since the insertion of the array into the scene requires a double exposure, two masks were prepared: one to mask out the scene and expose the array, the second to mask out the array and expose the scene. A registration bar and a punch were used to align the negatives, the masks, and the copy film. A strip of film with two register holes on it was attached to the original Libyan Desert negative. Both were held in position by the register bar. Above this was placed the unexposed print film, SO3404, which was also held in position by the register bar.

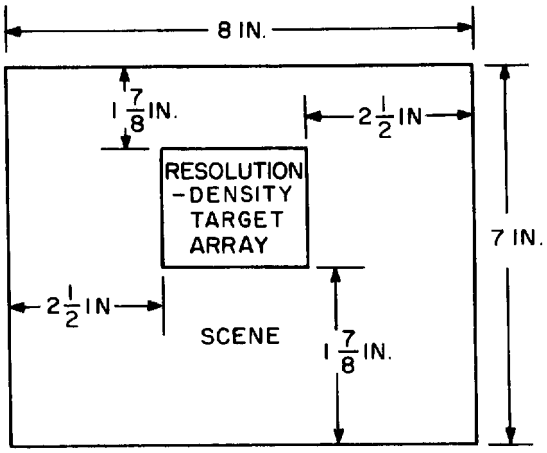


Figure II-3. Specimen Arrangement for Image Degradation Experiment

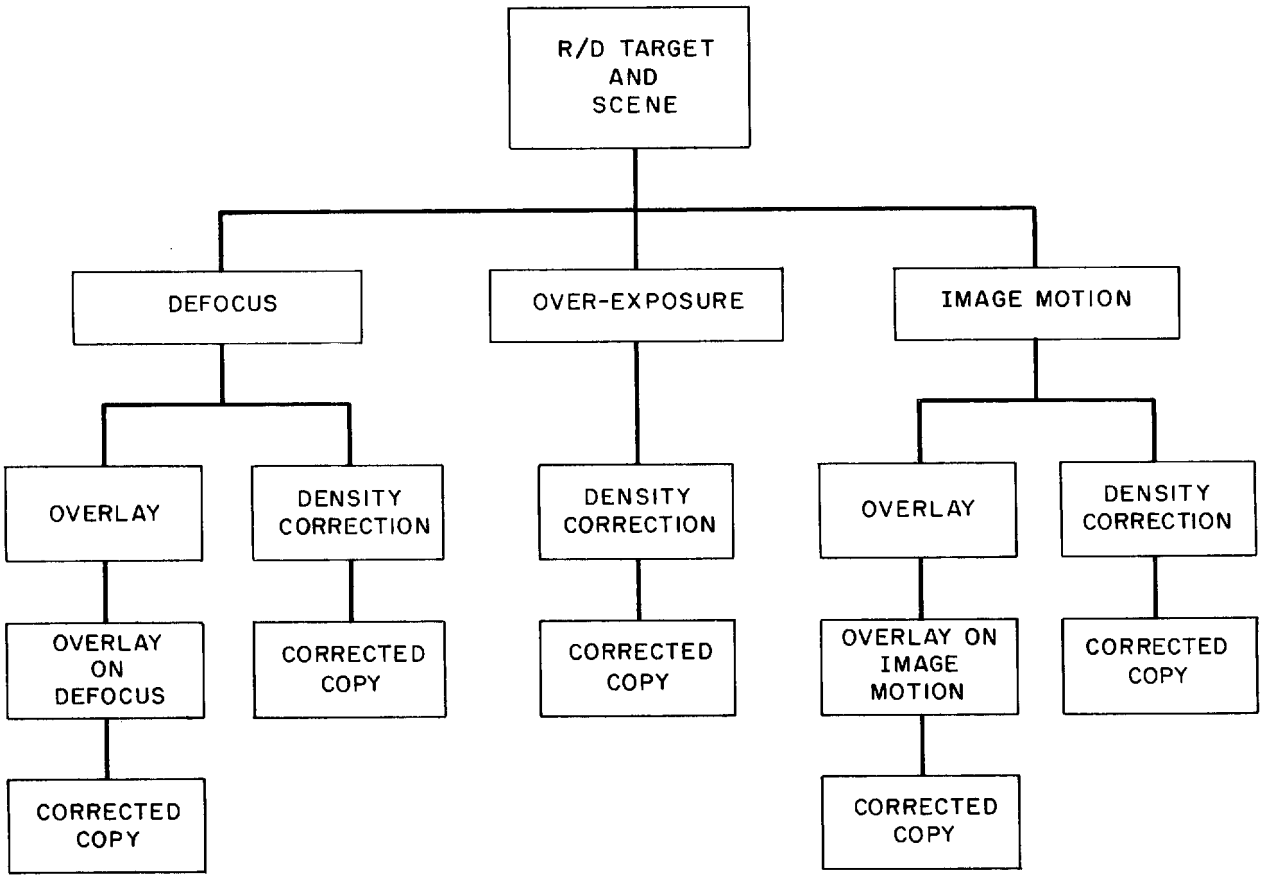


Figure II-4. Plan for Image Degradation and Correction

The transparancy which included the degradation of both the Libyan Desert and the triangle array was made on the HLC Dekagon copy camera where copy-to-film parallelism was carefully maintained. The camera was set as close to a 1-to-1 ratio as its limitations would permit. The transparency was given 4, 8, and 16 seconds exposures at f/8. SO3404 film was used to make the negatives, which were then processed in D19 developer. The standard exposure was 4 seconds and the overexposures were 8 and 16 seconds. Maintaining all camera conditions the same, with the exception of focus, a second negative was prepared. The lens-to-film distance was changed to obtain a $\Delta S'$ of 0.1 inch defocus.

A sample of image-motion degradation was also prepared on the HLC Dekagon copy camera. The effects of motion were simulated by moving the negative at a constant rate of 0.4 millimeter per second during the exposure time of 4 seconds. A motor was mounted on top of the illuminator that supported the transparency. Guides were placed on the sides of the illuminator to prevent the array from wobbling during the image-motion cycle. The diffusion plate was cabled to the motor by means of a pulley. The exposed film (SO3403) was processed in the same manner as previously described. The result was a one-dimensional image translation during the exposure cycle.

Microdensitometric traces for a segment in the scene for the standard, defocus, overexposure and image-motion specimens, are given in Views A, B, C, and D, of Figure II-5. Element a, as well as peaks on both sides, are density profiles of sand-dune crests. Although the high-contrast elements varied in contrast for the cases of defocusing, View B, and overexposure, View C, they were, generally, not lost. Defocusing tended to reduce contrast whereas overexposure tended to increase it. However, small low-contrast elements were smoothed out in both cases. Image motion, shown in View D, degraded the scene considerably more than either defocusing or overexposure. Low and medium contrasts were almost completely lost, and high contrasts were greatly reduced (but not at as high a rate of change as the lows and mediums). In addition, it can be noted that the image motion actually caused a shift in the position of some of the density peaks, as can be seen by comparing the position of a in View D with the position of a in the other three views.

b. Correction Program

In the overlay correction cycle, the 0.1-inch defocused negatives were selected to demonstrate the correction of degraded pictures.

Several overlay positives were made on SO278 Kodak fine-grain aerial duplication film. The prints were made on the [redacted] contact printer. Several exposure latitudes were selected to give prints with a gamma from 0.8 to 1.2. This gamma range was selected to prepare different masks at several

STAT

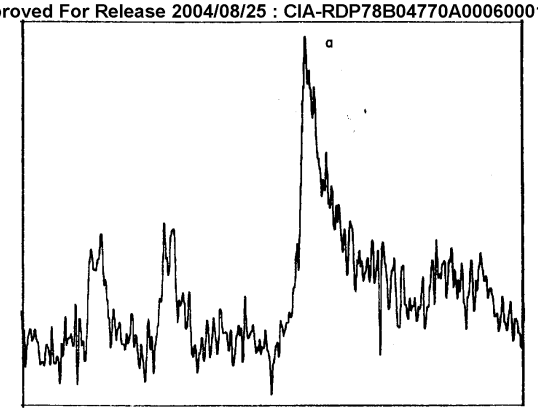


A. STANDARD

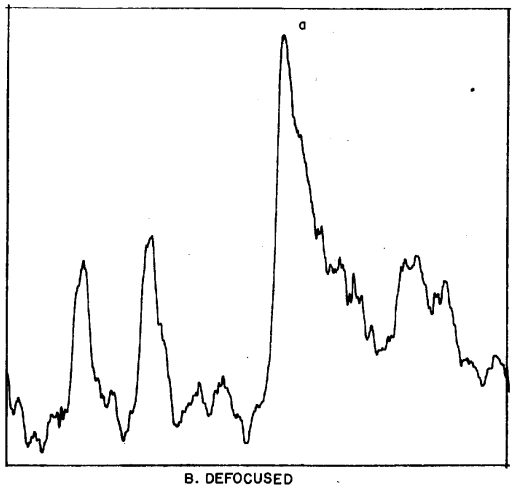


B. DEFOCUSED

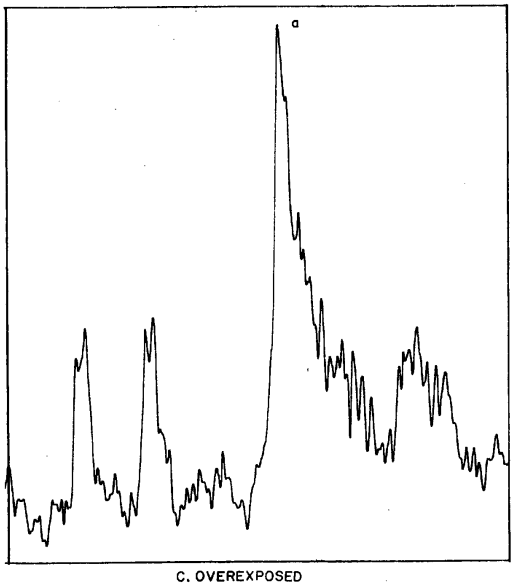


C. OVEREXPOSED

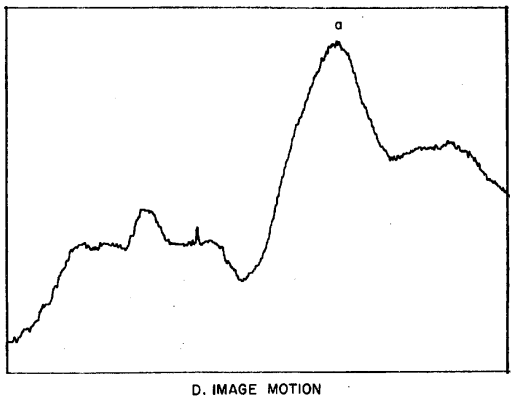


D. IMAGE MOTION

Figure II-5. Microdensitometer Traces for a Segment of the Sample Scene

different density levels (low to high densities) of the negative. The development time was kept constant. The prints were developed in D76, full strength, at 68°F. Eight ounces of anti-calcium per 32 ounces of developer was added to the developer to minimize the undesirable effect of the calcium precipitate during development. Each print was singly processed to assure uniform development. The selections of the proper masks were made according to the density levels of certain key images in the degraded picture and the spread of densities about these levels.

In the degradation, the density ratios of the defocused image had been reduced, shifting from high to medium or to low density. Consequently, image detail was subdued to a subliminal level of recognition. To control the density of the subliminal elements, a positive high-contrast mask was made. A negative-positive composite was made and held in register with the aid of the Kodak register bar. The composite permitted the further suppression of unwanted subliminal elements. The following effects were produced: (1) increase in contrast, (2) maintenance of the subliminal defocus densities in the subliminal level, (3) picture elements raised above the subliminal level.

An examination of the four microdensitometer traces of the standard and degraded pictures showed that the image elements of the sand-dune slopes and crests were clearly defined in the standard trace and degraded in the other three traces. There is a displacement of densities in the x axis so that low-resolution image elements are either barely noticeable or lost. In the correction cycle, the corrected image elements are those that are still present in the trace. The correction mask was used to increase the contrast of these picture elements above the subliminal level. A microdensitometric trace of another part of the scene shows a standard, defocused, and corrected composite picture element. The relationship between the standard, the defocused, and the partially corrected picture elements is shown in Views A, B, and C of Figure II-6.

In View A the picture elements of the standard scene of the Libyan Desert show a contrast ratio that brings them above the subliminal level. A careful look at the trace will reveal that the trace contains picture elements that are in the subliminal level. The contrast ratio is so low that these elements approach the threshold of sensitivity of the sensor, in this case, the microdensitometer.

The slopes of the trace in View B, representing the 0.1-inch defocused image, demonstrates the loss of contrast ratio between image elements as compared with the standard picture element. The trace in View B is relatively smooth; whereas, the picture elements in View A demonstrate marked differences between picture elements. Since the contrast ratio between picture elements in View B is very low, only the contrast range of the low-resolution image elements

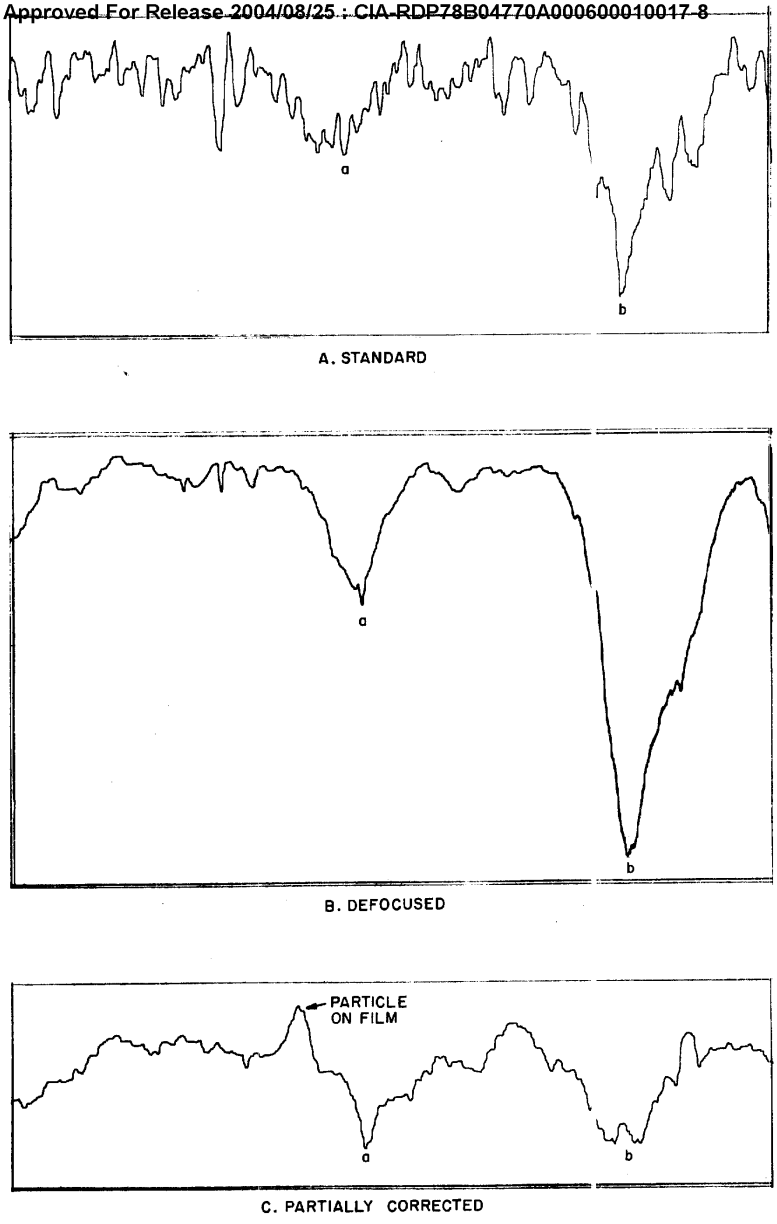


Figure II-6. Microdensitometric Traces Showing Relationship of Various Picture Elements

are discernible. A barely noticeable trace of other picture elements is left. There are extremely low contrast-ratio differences on the slopes of the trace. By increasing the contrast-ratio differences of these picture elements, the subliminal image elements rise above this level to the level of perceptibility. The partial correction of the image elements is illustrated by the trace shown in View C. This trace was obtained from the composite of a defocused negative and a positive overlay from which unwanted densities that contribute to the defocusing are suppressed. Curve elements b and c are sample regions in which the contrast change can be determined in the progression from the standard to the defocused and, finally, to the partially corrected copy.

Although the trace in View C does not approximate with the picture elements of the trace in View A, it does show that the picture elements that were not discernible at all are now forming ratios that indicate the presence of picture elements that were degraded as a result of defocussing. Further adjustment in masking is required to achieve a fully corrected image.

c. Conclusion

By proper correlation of masks to a given density level dispersed in a negative, a range of picture elements can be corrected by subsequent exposure of a number of mask-negative composites. Contrast ratios of densities can be varied to either suppress or accentuate to the level of perception.

The preparation of masks and composites is defined by (1) the accuracy with which proper registration is maintained, (2) the demarcation point of sharp and unsharp image-element components relating to imagery, and (3) the densities forming the background of the image to be corrected.

Correction of an image by means of overlay masks produces satisfactory results; however, it is time consuming. Further work is required to develop registration techniques and the development control of high-resolution image elements.

It is not possible to obtain good registration by use of EK registration. The registration bar does not permit good alignment due to the dimensions of the holes on the films and the pin diameter, as well as the location of the pins.

2. Operational Scenes

The customer furnished the aerial film from which images could be selected for elevation from a subliminal level to an information-retrieval level. The aerial film is identified as AFSPPL Mission Number 40-09112, and the film data is as follows:

a. Original Negative Film

(1) Type SO213

(2) Filter Wratten #12 (Yellow)

(3) Density

(a) Maximum 2.50

(b) Minimum 0.80

(c) $\triangle D$ 1.70

(4) Lens E.F.L., 24 inches

b. 2nd Generation Positive Film

(1) Type SO278 (Duplicating Film)

(2) Print Number 8

(3) Developer DD 1:1

(4) Control Gradient 1.04

The following frames and associated correction requirements were reviewed on the light box using the unaided eye as well as optical aids such as 7× and 20× to 50× magnifiers.

| Frame No. | Correction Requirement |
|---|---|
| 46413 | Image elevation relevant to the cloud area |
| 46414 | (1) Remove cloud shadow from houses<br>(2) Correct light-struck area |
| 46417 | Image elevation in light-struck area |
| 46443 | Remove cloud shadow over agriculture |
| 46574 | Elevate bar targets and imagery |
| 46889 | Haze compensation |
| 46894 | General image improvement |
| 46910 | Correct and compare with good frame |
| 46972 | Correct and compare with 46971 |

For the preliminary effort, a more detailed study was made of frame number 46572 which is very similar to frame number 46574. Two types of images were selected: a tri-columnar bar target and a single aircraft. The bar target contained elements that are subliminal. On the aircraft the service designation (USAF) was completely subliminal.

A correction plan was outlined in the following manner: The higher resolution elements of the bar target would fall into the low-contrast region. The basic correction is to change the low contrast to a high contrast, as defined in MIL 150-A specification. For the aircraft, density changes would be introduced to produce a high contrast between the service designation (USAF) and the wing of the aircraft. A medium contrast would be produced between the wing and the ground.

To modify density differences and density levels, two types of techniques were considered: The first technique is the use of an intensity-modulated CRT printer and the second technique involves the use of phase-amplitude modulation.

a. Intensity-Modulated CRT Printer

The printer was not available for use during this reporting period. Consequently, only a brief description will be given of the techniques that were expected to be used to modify the two selected images in the picture.

Since the CRT spot is relatively large with respect to high-resolution image-element dimensions, it is necessary to enlarge the image elements. To establish feasibility, a section of the frame whose dimensions are between one-half and one inch has been selected for enlargement on the HLC Dekagon copy camera so as to obtain a frame size of 9 × 9 inches for density modification programs. The printer will be used then in its intensity-modulated mode at several different modulation and exposure levels to determine the extent of image improvement that can be achieved through light modulation. After density modification, the 9 × 9 inch frames will be reduced to their original sizes for measurement and comparison. In this manner, the corrected transparency can be compared with the original. For medium and low-resolution image elements, the CRT printer will be used directly (without any enlargement of the original film) in the density-modulation printing. For several density differences at various density levels, specimens will be prepared for evaluation on a specific light box (Richards).

b. Principles of Image Formation

Another method for varying the contrast of micro-imagery is by the use of phase and amplitude control techniques. These techniques are used in the field of microscopy; the specific type of instrument employed is a phase-contrast microscope. The application of these techniques is generally related

to contrast improvement pertaining to visual inspection requirements. These basic principles of phase amplitude modulation are also applicable to aerial photographic printers.

The schematic diagrams in Figures II-7 and II-8 are intended to show the principle of image formation in a phase-contrast microscope system, and suggest how direct light (passing undeviated through the object structure) and the diffracted beams (deviated in passage through the object by the object structure and entering the objective) are made to recombine and form, through their interference effects, a representative image of the object in the final image plane.

The principles on which the phase microscope is based are shown in View A, Figure II-7. Light wave $a_2$ passes through a transparent object (d). Light wave $a_2$ has slowed down with respect to light wave $a_1$, which did not pass through the transparent object, and accordingly, the two light waves are out of phase. However, the eye and photographic films are insensitive to phase differences. Light wave $a_3$ passes through an absorbing medium (e) and is reduced in amplitude as shown. However, in contradistinction to phase differences, amplitude differences are visible. When light waves of the same phase and amplitude are combined in the image as shown in $b_1$ and $b_2$, they add to produce bright contrast (i.e., the image is brighter than its surrounding area). Similarly, dark contrast (where the image is darker than the surrounding area) can be obtained by producing light waves that are out of phase and amplitude with each other, as shown in $c_1$ and $c_2$, and combinations of amplitude and phase differences can be obtained that produce lighter or darker greys.

Light waves may be superimposed as shown in View B, Figure II-7. Section I shows that the wave P, resulting from a slightly retarding particle, as in curve $a_2$, may be broken into two waves, S and D. Section II demonstrates the effect of a bright-contrast diffraction plate using waves of the same phase and amplitude, resulting in a brighter image. In Section III the wave S has been partially absorbed, and wave D has been retarded, so that S and D are out of phase and produce a darker image.

The principle of operation of the phase-contrast microscope is shown in Figure II-8 (Reference 1). (The eyepiece, which primarily serves as a viewing magnifier, has been omitted.) An annular diaphragm to control the illumination on the object is placed in the lower focal plane of the substage condenser, and is imaged by the condenser and objective at the rear focal plane (exit pupil) of the objective. An annular phase-altering pattern (diffraction plate) is placed in this plane. As shown by the solid lines, undeviated light from the controlling annular diaphragm will pass through this annular phase-altering region and will effectively acquire an advance in phase of one-quarter of a wavelength of red light (as provided by a Wratten B (No. 25) filter) over that part of the light that is diffracted

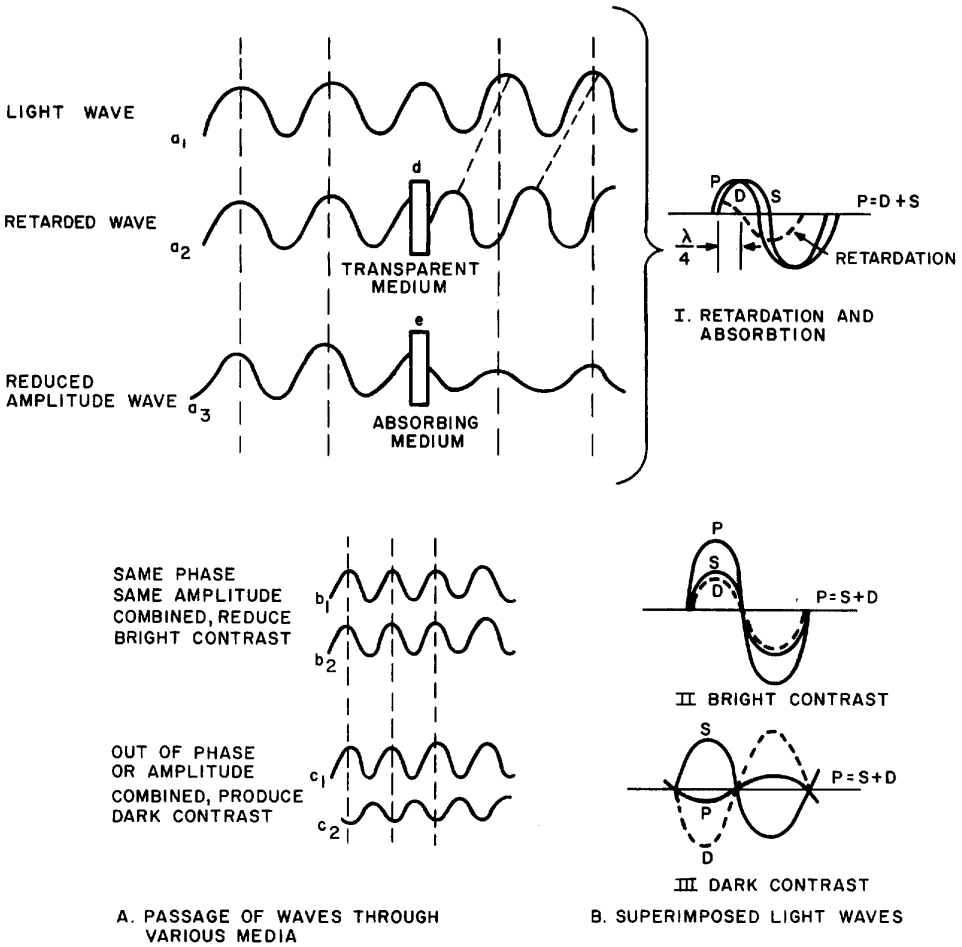


Figure II-7. The Principles of Image Formation in a Phase-Contrast Microscope System

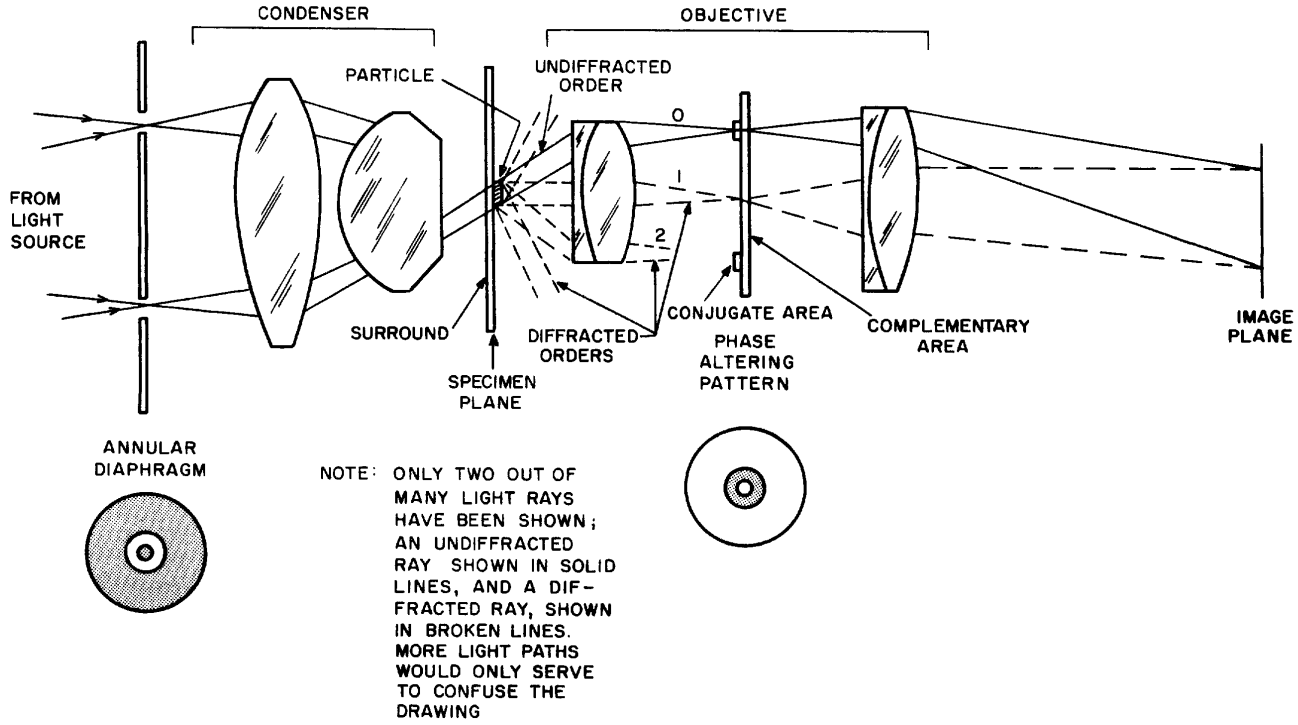


Figure II-8. Principle of Operation of Phase-Contrast Microscope

by the object structure (shown by broken lines), gathered by the objective, and passed through that region not covered by the phase altering pattern. The final image will be formed through the resulting interference effects between the two portions of light; alterations in phase relations in the illuminating rays, introduced by elements of the specimen material, will be translated into brightness differences by the phase-altering pattern. The resulting phase contrast reveals structural details through enhanced contrast.

The phase-altering pattern consists of optical glass on which is vacuum evaporated a very thin layer of metal, or a layer of a dielectric, or both. The layer of metal absorbs light, while the dielectric retards light. The layer of metal and/or dielectric must be of sufficient size to cover either the image of the annular diaphragm formed in the objective or the complementary area of the remainder of the objective. These layers act upon the direct light from the background and the deviated light from the specimen so that recombination in the image will produce visible phase or amplitude differences in the specimen. Typical array configurations are shown in Figure II-9.

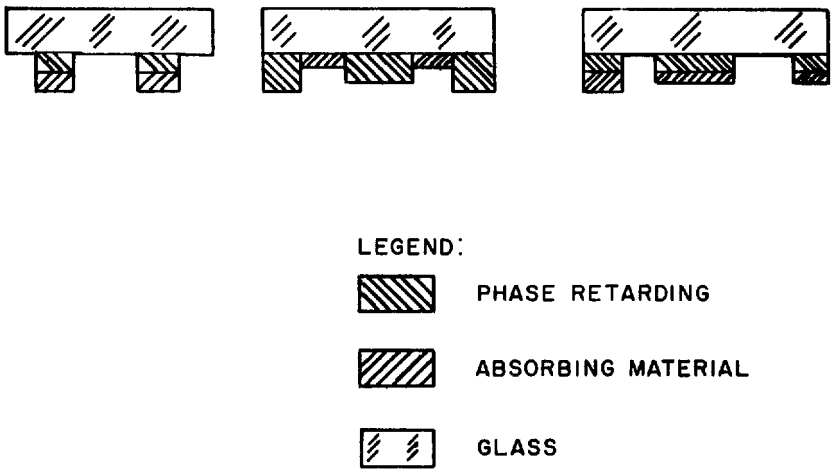


Figure II-9. Alternative Arrays for Phase-Altering Pattern

The bright-contrast diffraction plate absorbs, retards, or retards and absorbs the deviated light, but has no effect on the undeviated light. When the bright-contrast diffraction plate is used, regions of greater density in the specimen will have a greater optical path, and hence, will appear brighter than those of a lesser density, which, in turn, have a lesser optical path.

The phase-contrast objectives used gave positive, or dark, contrast. In the resulting phase image, regions of greater optical path in the object will appear darker than those of less optical path. Since the optical path, for light of wavelength lambda ($\lambda$), passing through a medium of refractive index n, and thickness t, is given by $nt/\lambda$, regions of equal thickness having a higher refractive index will appear darker than equally thick regions of lower refractive index. Regions of equal refractive index, but having greater thickness will likewise be darker than those having equal refractive index, but less thickness.

For the equipment used in the experiment the phase-contrast objectives introduced one-quarter wavelength of light phase shift when using the red light provided by the Wratten B (No. 25) filter. The use of other colored filters, although not restricted, will normally result in a departure from this amount of shift. The use of colored filters may prove to be of some advantage in enhancing contrast.

For the preliminary investigation, a [redacted] Dynazoom laboratory microscope with phase-contrast accessories and a modified 4 × 5 graphic-type camera was used for the replication cycle. On frame number 46572, it was noted that it was not possible, at any magnification (unity to 900×), to recognize either the service designation letters "USAF" on the wing of the four-engine aircraft or the medium- to high-resolution bar-target lines when the system was used as a bright-field microscope, using the [redacted] Dynazoom microscope. Using the [redacted] Dynazoom as a phase-contrast microscope, photographs were obtained containing contrast improvements that were useful in obtaining recognition levels of the subject matter. A total frame photograph whose primary purpose was to establish the location of the aircraft wing and the bar target is shown in Figure II-10. High contrast was introduced to obtain recognition of lines above 50 cycles per millimeter, as shown in Figure II-11. High contrast was established between the letters USAF and the wing, and with a limited effort, medium contrast was established between the aircraft wing and part of the airfield background, as shown in Figure II-12. The film used was 3404, processed in D19. The prints were produced on Kodabromide F-4 paper. This work was done on a time-limited basis and was intended primarily for demonstration purposes only. It is apparent that the picture quality could be further improved by grain suppression and better printing control.

STAT STAT STAT

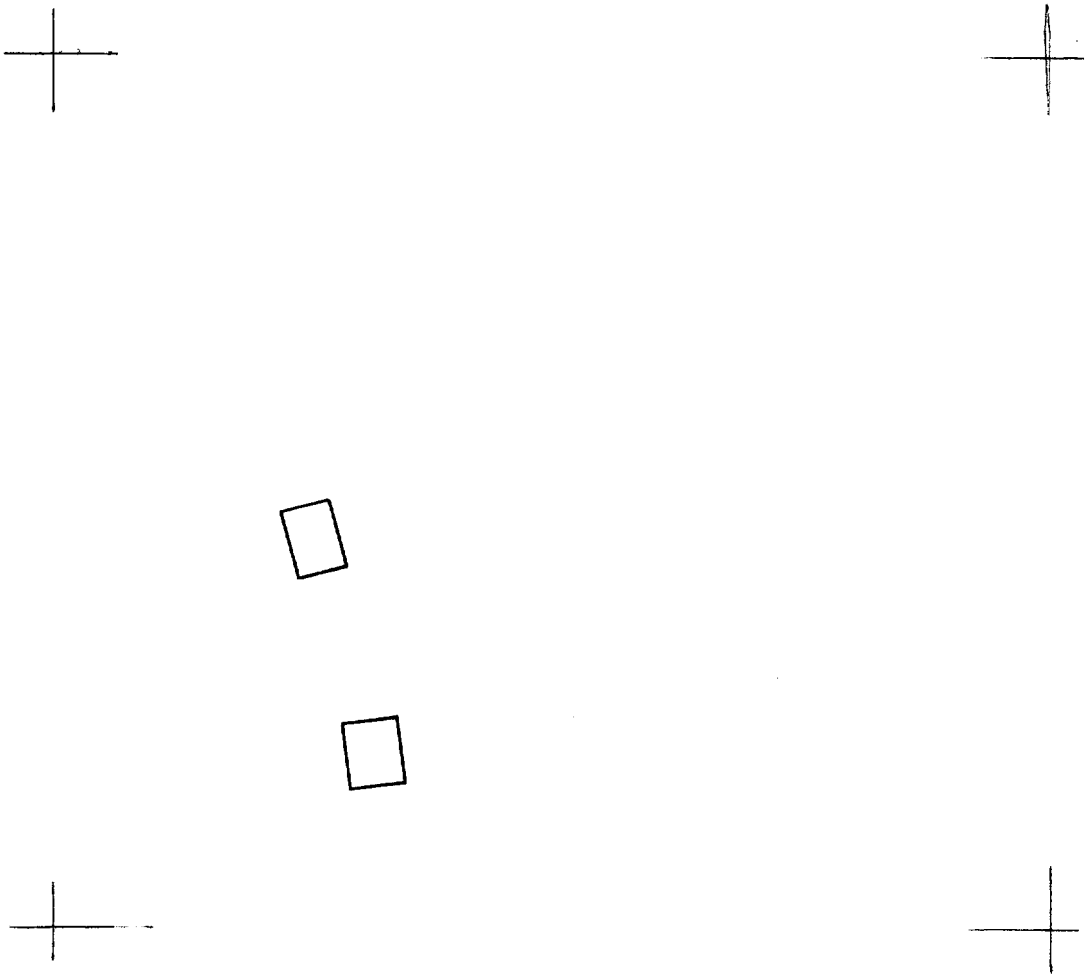

Approved For Release 2004/08/25 : CIA-RDP78B04770A000600010017-8

Figure II-10. Location of Airplane and Resolution Test Target in Frame No. 46572

A. Uncorrected

B. Corrected

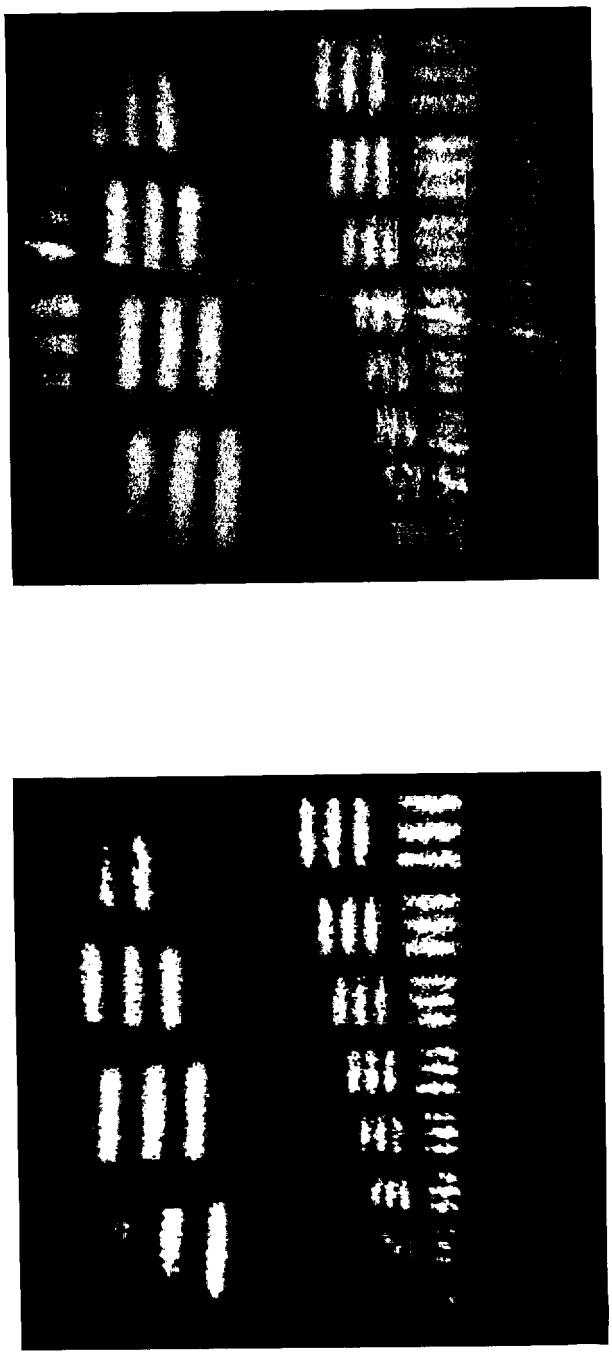

Figure II-11. Uncorrected and Corrected Images of Resolution Test Target

A. Uncorrected

B. Corrected

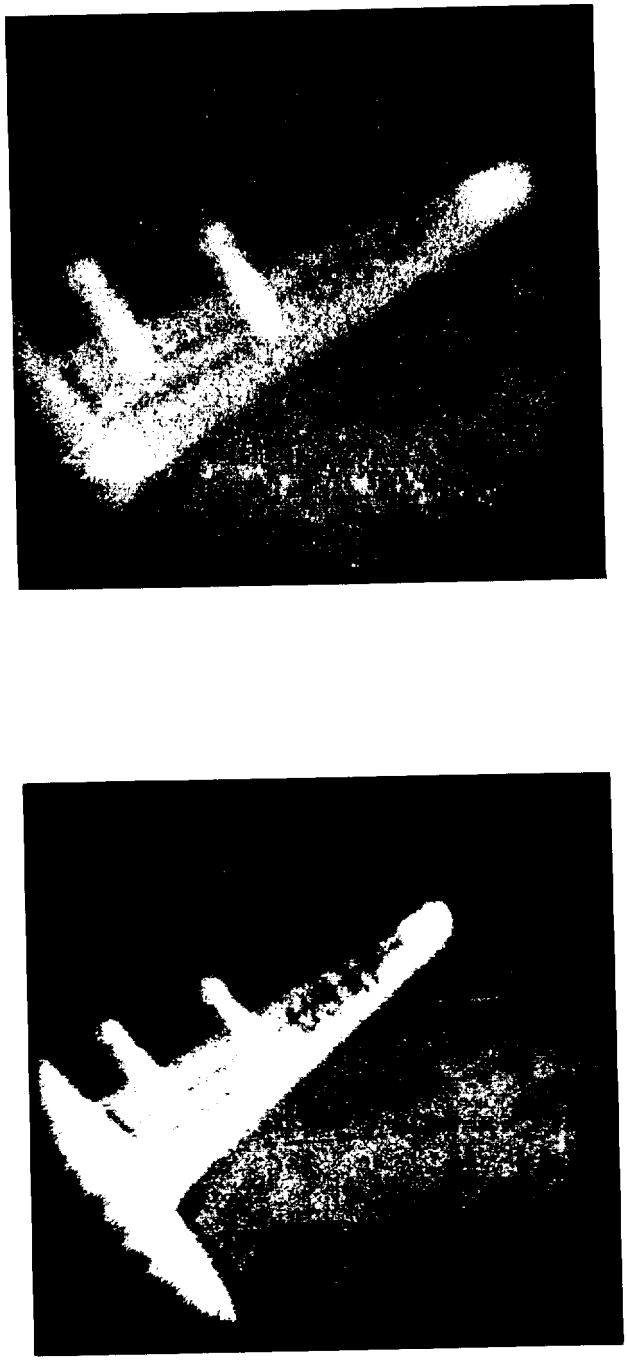

Figure II-12. Uncorrected and Corrected Image of "USAF" Designation and Wing-to-Background Contrast

With another method, called "Polanret", either phase shift or amplitude ratio can be varied; the diffraction plate is replaced by polarizing, analyzing, and birefringent retarding elements. It is suggested that further investigation be pursued in the development of a photographic contact printer of aerial film utilizing these as well as other basic principles. Furthermore, the phase shift and amplitude ratio should be programmed to operate together as a function of printing requirements. The printer can be either a slit or frame type.

During the next reporting period, the modulated-light CRT printer will be used for processing pictures. Pictures with different types of imagery under different conditions will be selected and their characteristics described. Various combinations of controlled printing and developing will be tried to enhance different features in the pictures. Analyses will be made of the resultant pictures using different combinations of processing, and a program of suggested processing sequences will be suggested according to the types of features desired and the picture characteristics. Reprocessing according to these programs will be done on the same or similar pictures to determine the validity of the program sequences and to simulate what might be done in an integrated processor.

## C. MODULATED-LIGHT CONTACT PRINTER

### 1. Description

The modulated-light contact printer developed under this contract was intended as a tool for use in various experiments in photographic image-modification techniques. It was expected that the photographic experiments would be dealing with high-resolution imagery, therefore, it was felt that the printer should provide a capability for high-resolution copying and manipulation (by means of modulated light) of spatial frequencies up to the neighborhood of a few cycles per millimeter. These requirements led to the two principal specification goals for the instrument:

1. High-resolution copying capability to the extent of 500 cycles per millimeter, or better, with suitable film.
2. Illuminating spot size of one millimeter, or smaller, at the film plane.

Other desired characteristics were:

1. Contrast compression of 30 to 1.
2. Illuminated area of 9 × 9 inches (at the film plane).

3. Isotropic scan to minimize the undesirable effects of exposure by a modulated scanning spot.

4. Provision for measuring the intensity of illumination impinging on the copy film, and if possible of viewing the exposing illumination (or a facsimile of it) for composing purposes.

5. Usefulness with a variety of copy films ranging in speed and opacity from Kodak (SO243) to gravure.

The mechanical arrangement devised to satisfy the requirements outlined above is shown in Figure II-13. Light from the five-inch diameter CRT is imaged onto the film plane in the film press. The maximum raster size on the CRT faceplate is 3 × 3 inches. Optical magnification ranging from 1-to-1 to somewhat more than 3-to-1 is available, permitting the printing of negatives in sizes up to 9-1/2 × 9-1/2 inches.

The light transmitted through the film press (which is the product of incident illumination, transmittance of the negative, and transmittance of the copying film) is converged by a Fresnel-type field lens, and then split into two paths by a semi-transparent mirror (60-percent reflective, 40-percent transparent). The transmitted portion is used by a photomultiplier tube to generate the feedback signal; the reflected portion is imaged onto a viewing screen. The operator views the screen from the side opposite to the direction of illumination, i.e., as in the case of a rear-projection screen. Two movable probes carrying small cadmium sulfide photo cells are positioned close to the illuminated surface of the screen. These probes can be moved to any point in the image. The light intensity measured by the probes is proportional to the light intensity incident on the corresponding region of the copying emulsion.

The intensity of the light at the viewing screen (as compared to that at the copying emulsion) is reduced by scattering in the copying emulsion, attenuation in the antihalation backing of the copying film, and the reflectance of the beam-splitting mirror. Therefore, the cadmium sulfide probes have been found to be most useful for measurements when relatively transparent copying films are used. When the attenuation of light to the viewing screen is too high, less direct methods of measuring the image-forming flux must be used. They might be used for initial measurements by (1) using no copy film at all, (2) using a piece of exposed test film in the film holder along with the negative, or (3) using a chip of test film in front of the photomultiplier, and no copy film in the film holder.

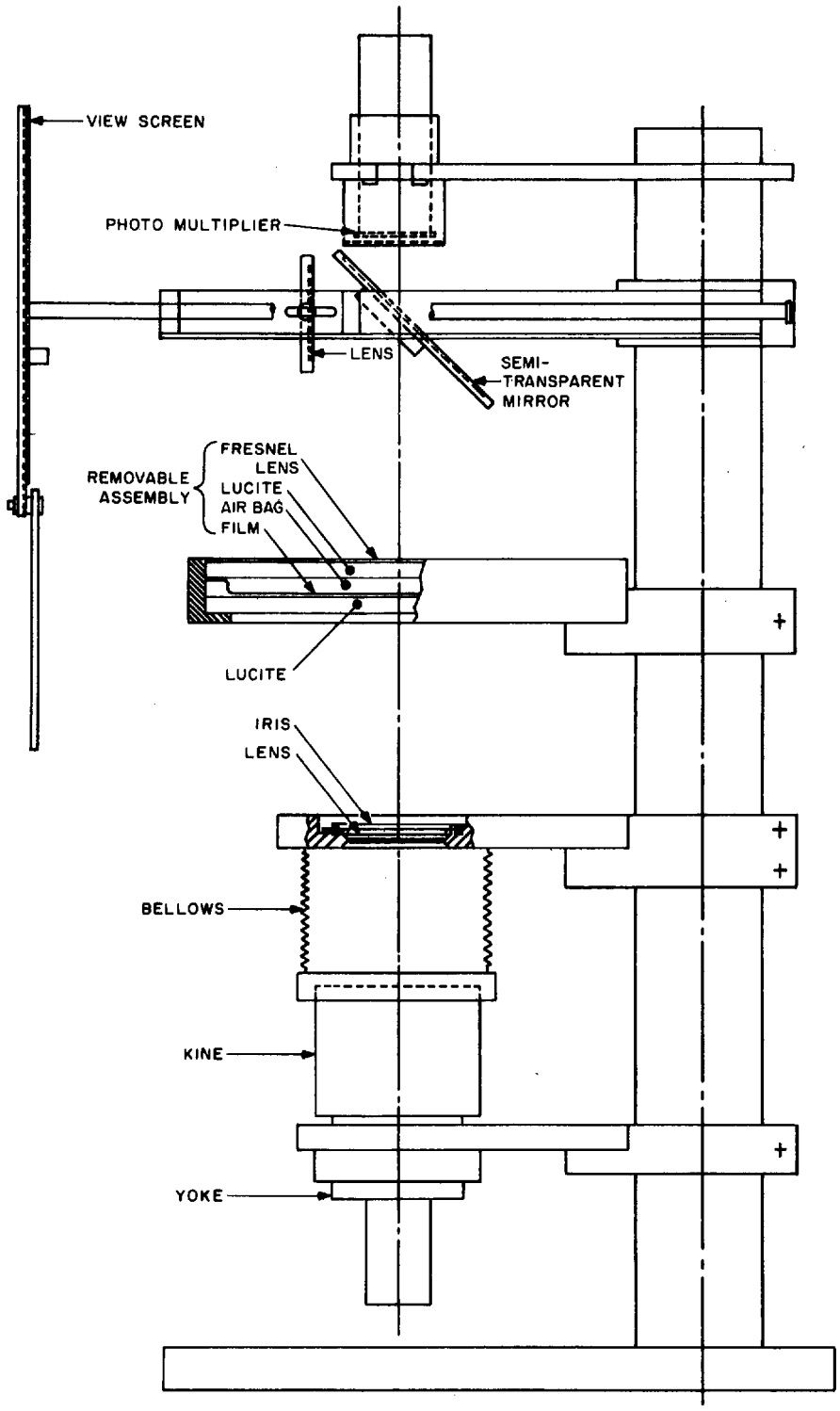


Figure II-13. Modulated-Light Contact Printer, Mechanical and Optical Layout

The photomultiplier, lens-and-mirror assembly, film press, and cathode-ray tube assembly are each mounted on heavy brackets which are, in turn, mounted on a heavy drill press mount. This mounting scheme provides solid vibration-free operation.

The film press consists of a lower transparent plate of 1/2-inch thick Plexiglas on which the films are laid. A pressure bag of transparent Saran film supported by another 1/2-inch thick Plexiglas plate forms the top of the press. The Fresnel field lens is mounted directly over the upper Plexiglas plate.

It is expected that the capabilities of the printer will be fully measured early in the next reporting period. These measurements will include, for combinations of different exposure levels,

1. Uniformity of illumination across the film,
2. Density-matching capability,
3. Effects of format and spot-size changes, and
4. Printing resolution.

Upon completion of these measurements the printer will be utilized in the exploration of electrical-chemical processing techniques.

## 2. Resolution

The illuminating spot at the film plane can be reduced to a diameter of less than 1 millimeter with a magnification of 3-to-1.

The contact printing resolution was calculated from geometrical considerations to be greater than 660 cycles per millimeter for emulsions of 5-micron thickness. Tests were made with a test pattern on a Kodak High-Resolution Plate having approximately sinusoidal patterns up to 200 cycles per millimeter. The results of these tests, conducted (on SO243), demonstrated resolution performance commensurate with that obtained with a [redacted] printer, Model No. 1119, which has demonstrated printing resolution greater than 500 cycles per millimeter. This test is indicative of the capability of the developmental printer, but not conclusive. The tests will be repeated using test patterns of higher spatial frequency recently supplied by the customer.

STAT

3. Modulation Tests

Quantitative tests have been made of the modulation obtained in the following three cases: (a) No copying film in press, (b) SO243, (c) gravure.

In each case, the test pattern was a step tablet having a minimum density of 0.05 and a maximum density of 3.02. There was also a completely opaque mask.

By use of a 50-percent beam splitter, the output of the kinescope was displayed on a temporary screen to the side of the printer. Measurements were made on this screen of areas of the test pattern and opaque mask that corresponded to maximum and minimum density. The beam splitter was placed at a 45° angle between the film press and the face of the kinescope, thereby, making it possible to measure the modulation of illumination without interrupting the feedback path. Both the gain in the feedback loop and the brightness level were adjusted for each case to give the same incident intensity on the opaque mask and the maximum modulation obtainable before system oscillation was encountered. The results of the measurements are given in Table II-1.

TABLE II-1. MEASUREMENTS OF MODULATION OF ILLUMINATION

| Condition | Region | | |
|---|---|---|---|
| | Opaque Mask | D=3.02 | D=0.05 |
| Test pattern with no copy film | 215 | 130 | 5 |
| Test pattern with SO243 | 225 | 85 | 4 |
| Test pattern with gravure | 225 | 100 | 9 |

In actual practice, proper exposure for films of different sensitivities would be obtained by either adjusting the brightness of the illumination or the number of scans in the exposure, or both.

It should be noted that circuitry is provided that permits exposures in integral numbers of scans. Each scan is of one second duration, and the scanning-line density is 2049 lines per picture diagonal. The scan pattern is an isotropic "box scan" in which each area is scanned in four directions.

The circuitry has been described in somewhat more detail in Reference 2.

4. Uniformity

Measurements of uniformity of illumination were made under conditions of no modulation and rapid scan, using a CdS cell 1 inch above the film plane. These results are presented in Figure II-14, Views A and B. The units are arbitrary. It is to be expected that uniformity should be improved with modulated light, since this mode of operation seeks to equalize illumination at all points. Measurements of uniformity at the film plane in the modulated-light mode could not be readily made, however, because insertion of a measuring probe would disrupt the optical feedback path.

5. Controls

The controls to the modulated-light contact printer consist of two groups: raster controls and modulation controls. These two types of controls are discussed separately in the paragraphs that follow.

a. Raster Controls

(1) Size and Centering

The size and centering controls for the x and y coordinates control the size of the raster from practically zero to somewhat more than 3 × 3 inches (on the CRT face). Both size and centering are independently controlled in each axis.

(2) Scan Mode

Selection may be made between a frequency-locked scan mode, which gives a frame rate of 1 frame per second, and a variable frame rate. The latter is used when a faster frame rate is desired for visual observation. The frequency-locked mode is used when exposing film.

(3) Exposure Selector

A selector switch is provided that permits exposures of 1, 2, 3, or 4 complete frames. This is operative only when the scan is in the frequency-locked scan mode.

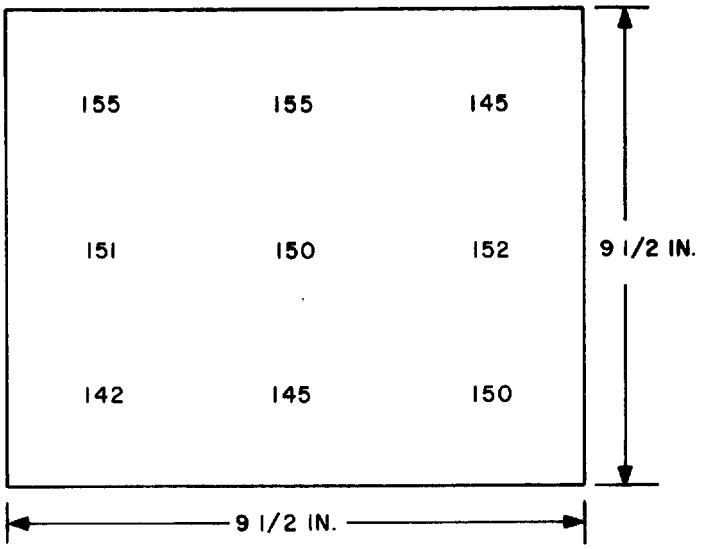


A. LENS OPENING 2 3/8 INCHES

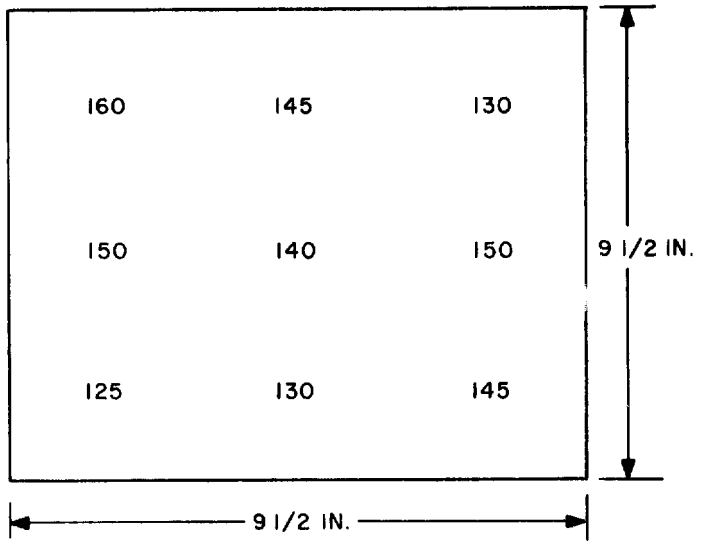


B. LENS OPENING 1 1/2 INCHES

Figure II-14. Measurements of Uniformity of Illumination with no Modulation (arbitrary units)

b. Modulation Controls

(1) Brightness

This control sets the d-c level of the CRT grid.

(2) D-C Level Control

This control sets the zero-signal operating point of the output amplifier, which drives the CRT cathode. Used in combination with the brightness control, it can be used to set the unmodulated CRT brightness level. By proper adjustment of these two controls, the modulation may be made to be non-linear for either very dense or very thin areas of the negative.

(3) Modulation Gain

There are two controls for modulation gain: one control regulates the supply voltage applied to the photomultiplier, and the other control regulates the gain in the transistor amplifier. These two controls operate essentially in series, and have the same function, i.e., control of the gain in the feedback loop.

(4) Auxiliary Controls and Adjustments

Mechanical adjustments are provided so that the magnification of the CRT raster can be varied from a ratio of 1 to 1, to somewhat more than 3 to 1.

(5) Focus Control

A control is provided for electrical focus of the scanning spot on the CRT. It may be varied from about 1/3 millimeter to about 5 times as large.

(6) Photocell Probes

A separate meter with dark current compensation is provided for measurement of the photocurrent (and hence incident light intensity) for each of the two CdS photocells. Currents ranging from 1 to 500 microamperes can be read by these meters in three ranges.

# SECTION III

# ELECTRONIC PROCESSING TECHNIQUES

The objective of the Electronic Processing Techniques portion of the program is to develop electronic image-processing techniques that will lead to photographic records with improved image perceptibility. Experiments to date have been conducted on a low-resolution breadboard. Experiments during the next reporting period will be conducted on a high-resolution breadboard.

## A. REVIEW

During the first reporting period, a preliminary electronic image-processing study was performed to identify the critical aspects of the proposed two-kinescope system. A preliminary breadboard electronic image-processing system, incorporating standard kinescopes, conventional beam scan, and broadband negative and positive feedback was then designed and constructed, using existing [STAT] -owned equipment. Experiments were performed to obtain answers to certain fundamental questions relating to the two-kinescope system:

1. Effect of the sensing light dilution on system operation,
2. Stability of the system using color separation,
3. Signal-to-noise ratio of the system,
4. Degree of registration obtainable with the two kinescope rasters, and
5. Shape of system transfer characteristic.

Based on the results of these experiments, the high-resolution equipment was designed, and the Ferranti equipment, needed to effect the breadboard change-over from low to high resolution, was ordered.

A block diagram of the low-resolution experimental setup is given in Figure III-1. The sensing kinescope scans the original photographic transparency with a fine spot of violet light at a low intensity. This light passes through the copy film and is picked up by the multiplier phototube and an electrical signal is generated. This signal is amplified, processed, and applied to the modulating kinescope. The fine-spot yellow-green light generated by the modulating kinescope exposes the copy film through the original transparency. The minus-yellow filter prevents the yellow-green light from reaching the multiplier phototube and causing system oscillation.

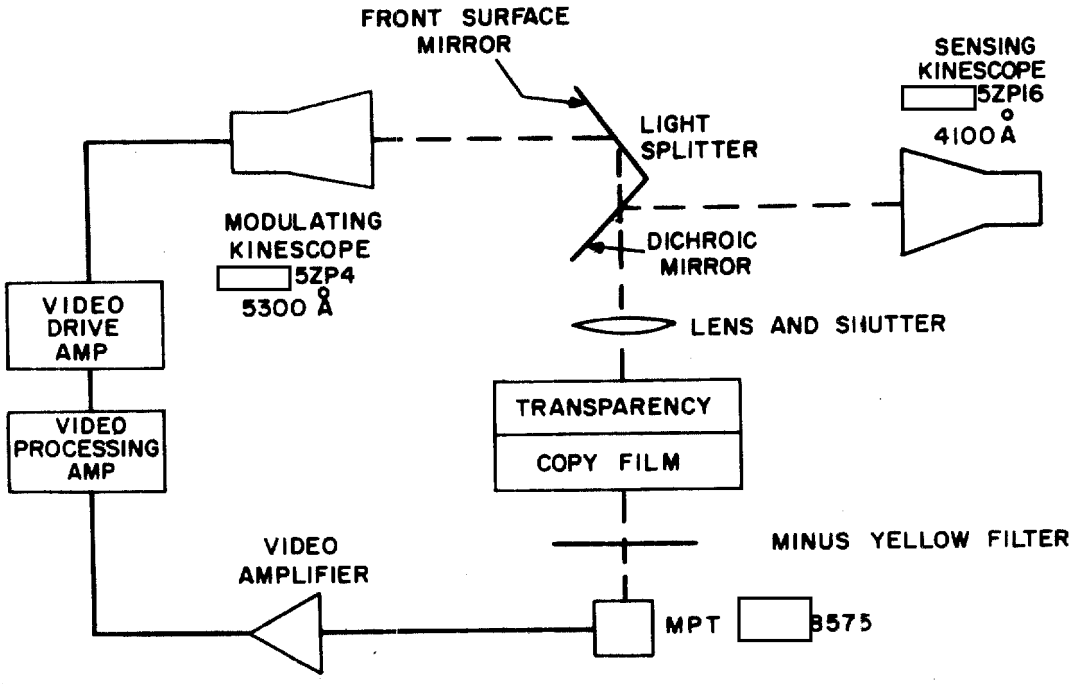


Figure III-1. Breadboard of Low-Resolution Electronic Image-Processing System, Block Diagram.

The amount of exposure given to the copy-film emulsion depends on the product of the transmittance of the negative and the sum of the sensing and modulating illumination. The exposure, in this process, is performed from point to point, sequentially, as the transparency is scanned by the light.

Compensation for the propagation delay between the two scanning beams is made by a slight shift in the horizontal centering of one raster with respect to the other so that the light from the modulating kinescope passes through the same portion of the transparency as the corresponding light from the sensing kinescope.

Deflection is the same for the two kinescopes, each of which employs sawtooth (unidirectional) scanning at conventional TV rates: H = 15, 750 scans per second, and V = 60 fields per second or 30 frames per second interlaced.

Pictures were taken during the first reporting period to establish exposure time and photographic development procedures. Although it was impossible to maintain registration of the two kinescope rasters over the whole picture, in the areas of good registration, there was evidence of improved image perceptibility achieved through the use of negative masking.

Since one of the advantages of the open-loop feedback system is the ability to use either positive or negative masking, or a combination thereof, experiments were undertaken to explore the relative merits of these possibilities. The results of the experiments are described in the paragraphs that follow.

## B. EXPERIMENTS WITH LOW-RESOLUTION BREADBOARD

### 1. Experiments with Positive and Negative Masking

The first experiment used high- and low-pass filters to reduce large-area contrast and at the same time further accentuate edge contrast. The video amplifier, as shown in Figure III-1, was replaced with the circuit shown in Figure III-2.

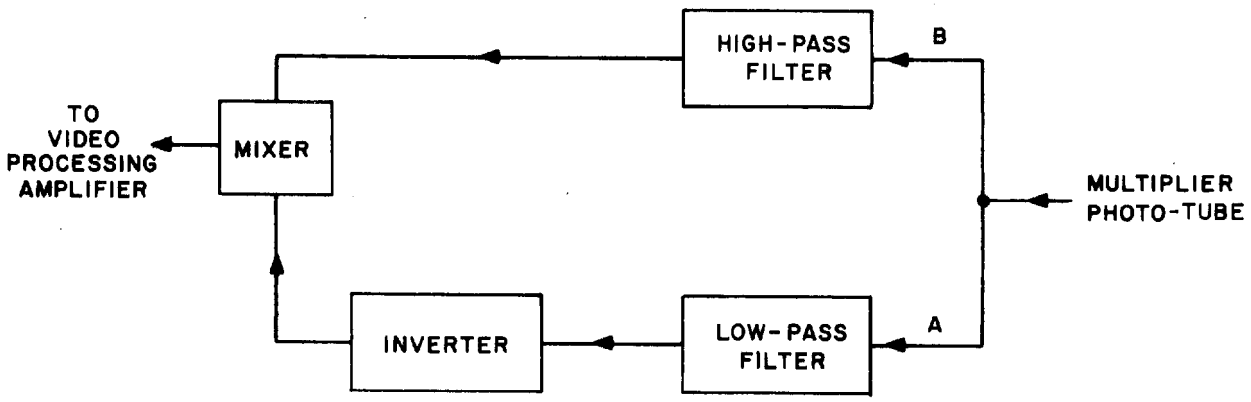


Figure III-2. High- and Low-Pass Filter Experiment, Schematic Diagram

The characteristics of the filters could be changed over various parts of the 20-megacycle video band. Either polarity was available for mixing. The low-pass filter, Channel A, would simulate the lower-resolution negative-mask signal, and the high-pass filter, Channel B, would produce signals in a positive polarity. When mixed, and the combination used as a light mask, it was expected that edge contrast would be increased due to the positive mask and large-area contrast would be reduced due to the negative mask.

The first anomaly to occur was that the conventional TV processing amplifier, used to restore the d-c component of the video signal, tried to restore the low-frequency signals that were lost in Channel B, the high-pass filter. Since these low-frequency signals were of the opposite polarity to that produced in Channel A, the negative-mask signal, some of the low-frequency signals making up the negative mask were cancelled.

To remedy this situation, it would have been necessary to mix the signals from Channel B at a point in the video chain beyond the processing amplifier. Obtaining such a high-level mixer would require the building of another wide-band video amplifier with considerable gain and power capability. This possibility was bypassed in favor of other experiments. Consequently, the results of the first experiment were inconclusive. The experiment will be repeated during the next reporting period with the high-resolution setup, which is equipped with the proper mixing arrangement.

Experiments were continued using edge-enhancing techniques, only. There has been considerable debate in the past as to which derivative (the first or the second) of the edge signal is more desirable for adding to the original edge signal to achieve increased edge contrast. Theoretically, the second derivative should be more desirable since it operates symmetrically on both the light and dark side of an edge, as shown in Figure III-3.

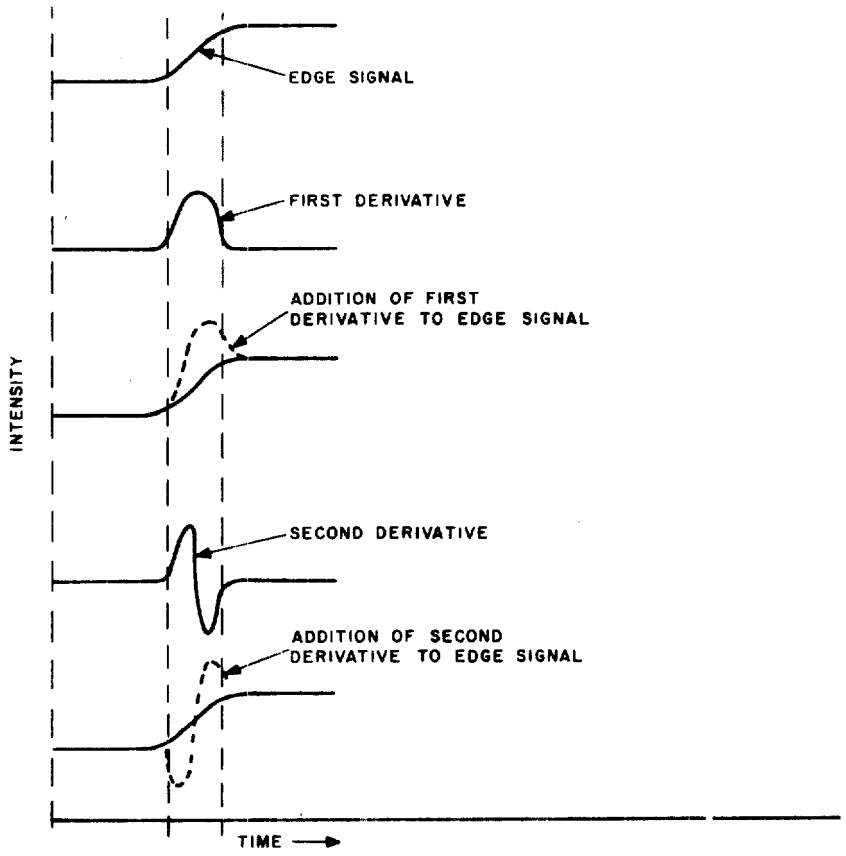


Figure III-3. Waveshapes for Second Derivative Addition to Edge Signals

To obtain the effect electrically, high peaking of the video circuitry would be required to the extent that an increase in the noise would result. Such circuits were tried and it was found that the initial signal-to-noise ratio of the system was not high enough for the second derivative signals to exceed the noise sufficiently. Although the polarity of the second derivative signal (pulse noise) is opposite that of the original edge signal (plus noise), the added noise was greater than the original, and, therefore, the resultant noise was greater than the original.

Polarity reversal, or noise cancelling, systems were considered next. However, these systems usually cancel the useful signals at the same time. If the effect of differentiation could be achieved without the additional amplification required with conventional differentiation, the noise level would be that of the original system for the part of the spectrum considered. The system described in the paragraphs that follow achieves this result.

The waveshapes for conventional and delay-line differentiation are shown in Figure III-4. A block diagram of a delay-line differentiator is shown in Figure III-5.

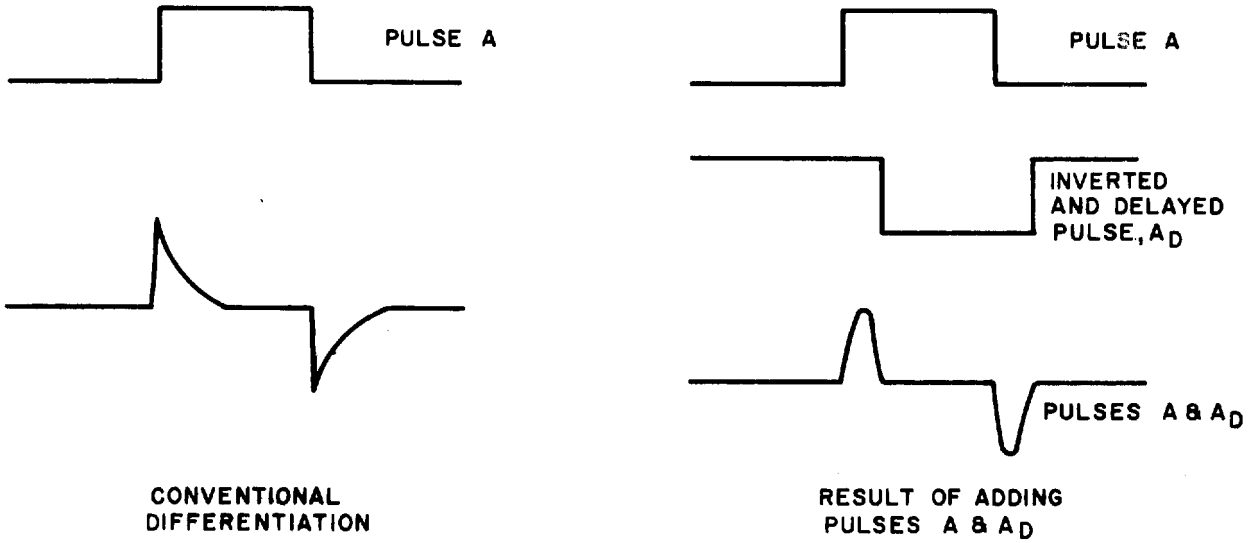


Figure III-4. Waveshapes for Conventional and Delay-Line Differentiation

If two identical video amplifiers, A and A', are connected with a wide-band delay-line and inverter in series with one or the other, an effect of differentiation is achieved when the delay is varied from the point of complete cancellation. If pulse A is inverted and delayed, and the resulting pulse, $A_D$, is added to A, pulses $A+A_D$ are obtained. Since the width of pulses $A+A_D$ is changed by changing the delay, the amount and character of the noise changes; the wider the pulses, the larger the grains of noise. As the pulses are narrowed to that required to put a fine white edge on a black object, or vice-versa, the noise

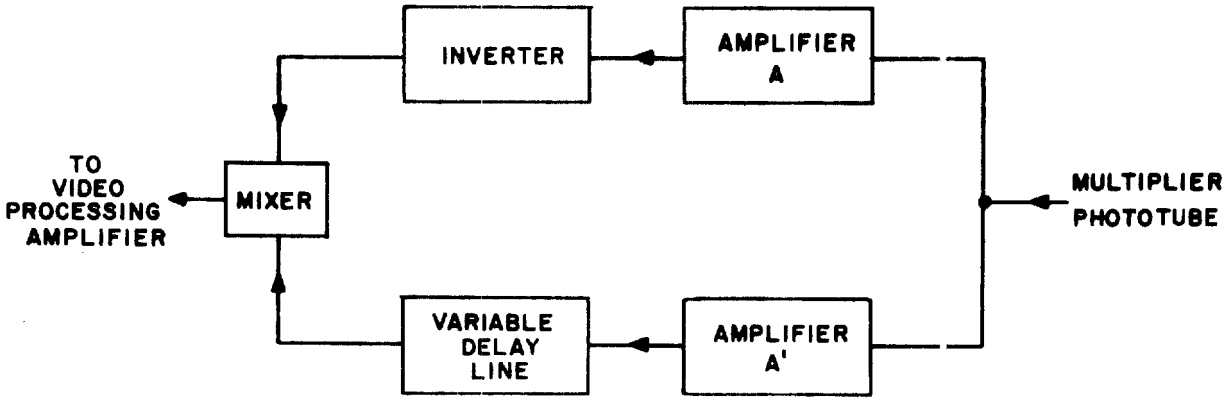


Figure III-5. Delay-Line Differentiator Circuit, Block Diagram

appears to be less due to its being fine grained and therefore less noticeable with a given bandwidth system, although it is still present. Changing the delay acts as a change of the pass characteristics of a high-pass filter.

The delay line used was a type 606-S, made by [redacted] STAT N.J., which had a delay of 0.5 microseconds. A test of the effectiveness of cancellation is how nearly the resultant approaches zero when the delay is the same for each channel. The cancellation could be made almost perfect in this experiment, the only signals left were some very fine edges that looked like second derivatives of edges.

Since this technique appeared to be an improvement over conventional differentiation plus amplification, pictures were taken without negative masking over large areas but with positive masking for edges only, as shown in the two views in Figure III-6. The positive edge-masking effect was added to a d-c level (from the sensing light and the d-c restoration circuit) to expose the full scene.

Comparison of Views A and B in Figure III-6 shows that the difference in results with and without positive edge masking is marginal. The overall contrast is a little greater in View A, due to positive masking not only of edges, but to a small degree, of the entire scene. The enhancement of the edges in View A is dependent on accurate registration of the light mask and the transparency. Slight misregistration can cause the edges of the processed picture to look less sharp than those of the unprocessed picture. An improved, a more rigid base for the test setup is indicated.

As a result of a suggestion by the Customer, during a visit in January 1966, experiments are currently being concentrated on negative masking only. More pictures to demonstrate results were requested by the Customer. Over 200 pictures were made to demonstrate and verify the effects achieved when using

negative masking only, of (1) gray scales of known transmission, (2) triangular wedges of known edge focussing, (3) dot patterns, and (4) scenes from different parts of a positive transparency of the Virgin Islands. Each of these picture-making sequences are described, and the results illustrated, in the paragraphs that follow.

2. Experiments with Negative Masking Only

a. Gray Scales

Gray scales of known density, or transmission, help establish the gamma of a TV system. In the system described under Paragraph A of this section, a light area in the transparency, which requires a darker mask behind it, will always print lighter than the mask predicts because of the addition of the unmodulated sensing light. In the dark areas, the brighter mask will be a little brighter than predicted for the same reason. This non-linear effect may be compensated by shaping the transfer characteristic, although this has not yet been done.

Another reason for the transmission of too much light through the light areas of the transparency is insufficient video drive on the modulating kinescope. Based on the darkest step (brightest mask), the lightest step (darkest mask) prints even lighter due to the masking light not having the same overall range as the measured range of the gray scale. The indication is that the modulating kinescope is not being driven sufficiently far in the direction of cut-off.

The joint effect of both these phenomena, shown in View A of Figure III-7, can be compared to View B, which is an unmodulated print of a 16-to-1 gray scale.

By separating these phenomena and making intensity measurements on the resulting pictures, the gray scales can be utilized to help determine the needed modifications in the design of a printing system or in its proper tuning. In particular they can be used to determine the shape of the transfer characteristic of the open-loop TV system to compensate for (1) the non-linear effect on exposure of the contact transparency due to the addition of the sensing and modulating lights and (2) the amount of video drive needed on the modulating kinescope.

b. Triangular Wedges

Test patterns with edges having known amounts of edge defocussing are used to study both the theoretical and the practical aspects of edge processing, using the negative masking technique. They may be made in different shapes for various applications. Triangular wedges were used for this application because they were readily available.

Edge processing is associated with the amplitude and width of the edge overshoots. Overshoots are defined as the departure from the original edge-signal waveshape, where, just before an edge is reached in a dark area, the signal goes a little darker, and after passing to a light area, it goes a little lighter. They are caused by the finite size of the sensing spot, which, when close to an edge, illuminates some area on the opposite side of the edge from where it is nominally pointed. Hence, the total light sensed is greater than it should be when passing from light to dark across an edge, and vice versa. This is similar to adding the inverted second derivative of an edge to the original edge signal. A mathematical analysis of overshoots is given in Section IV, "Techniques Analysis."

Pictures of triangular wedges for the cases of both sharp and defocussed edges are shown in Figures III-8 and 9; Figure III-8 includes a comparison between the results of scanning both perpendicular and parallel to the wedge. This experiment represented an attempt to see if there were any adverse effects due to unidirectional scanning. There are differences in the overshoots, but it is difficult to say whether they are due to the direction of scanning or to misregistration.

Views C and D of Figure III-8 show the effect of negative masking on defocussed edges. Here, the wedge is essentially perpendicular to the scanning. The overshoots are of less amplitude, but wider than for the sharp-edge wedge.

Views C and D of Figure III-9 show the effect of running a processed negative through the system a second time. Edge overshoots increase in amplitude due to the second negative masking process, as may be seen by comparing View A with View C.

All these pictures have been helpful in studying overshoots at edges. Overshoots are useful to increase edge contrast. Edge contrast may be increased with repeated applications of negative-mask printing.

c. Dot Patterns

The dots on the dot patterns used for the experiment were 0.01-inch in diameter and 0.04-inch apart, before enlarging 3 to 1. These dot patterns are used to check the registration of the system. Some of the dots in View A of Figure III-10 are not accurately registered. The misregistered dots show white "flares" on one side only. Registered dots show a little white overshoot equally spaced all around the dot. Measurements can be made of the amount of overshoot and the distribution of the misregistration through the picture. This information can be then used to help determine the cause of misregistration and the degree of correction needed. For example, in a unidirectional scan system, a delay appears as a uniform white flare across the picture on one side of each dot. In a box-scan system, a delay would appear as a large halo around each of the dots in the picture.

d. Aerial Photographs

Figures III-11 through III-15 consist of photographs of parts of a positive, 9- by 9-inch aerial transparency. These photos show the effect of negative masking over the areas of good registration, which include most of the central area of each photo.

They cover areas having one-inch diameters and are enlarged optically 3 to 1 directly on positive hard copy. The step from the contact negative to positive transparency was omitted for the purposes of this report. The resolution of the mask is about 10 cycles per millimeter for all the photos shown in this section of the report. The gamma of the TV system is also the same in the case of all photos in this section.

Scene types were chosen to show the effects of negative masking on (1) large and small light areas, (2) large and small dark areas, (3) city streets, and (4) wooded areas. The difference between the resolution of the contact transparency and the light mask that produced it is shown in the comparison between Figures III-14 and III-15. All photos using negative masking in this report were made using a similar mask resolution, 10 cycles per millimeter.

3. Conclusions

Pictures taken on the low-resolution breadboard did not show that those taken with positive edge masking only, provided sharper edges than those taken with overall negative masking. In a high-resolution system, with better registration than the low-resolution system, the difference may be more apparent.

Judging from the width of the overshoots on calibrated edge patterns, higher mask resolution may be helpful, and with the new setup, higher mask resolution will be available.

Since scanning lines are visible in some of the pictures, the use of either a higher number of scanning lines or a large scanning spot is indicated as a remedy. Increasing the spot size will decrease both vertical and horizontal resolution. An alternative would be to elongate the spot vertically without changing the horizontal resolution by a technique called vertical spot wobble. To achieve this a small auxiliary yoke excited by a current at a frequency higher than the highest video frequency would be used.

The two-kinescope system works well from the standpoint of stability and serves as a flexible laboratory tool. However, the rasters do not stay in register. The high-resolution breadboard is expected to be more capable of maintaining registration. Without having finished and tested the high resolution breadboard,

A. Positive Edge Masking

B. Without Positive Edges Masking

Figure III-6. Reproduction of Aerial Photo With and Without Positive Edge Masking

A. Negative Masking Only

B. Without Negative Masking, but Using Unmodulated Light from Yellow-Green Kinescope

Figure III-7. Gray Scale, 16-to-1 Transmission Ratio, With and Without Negative Masking

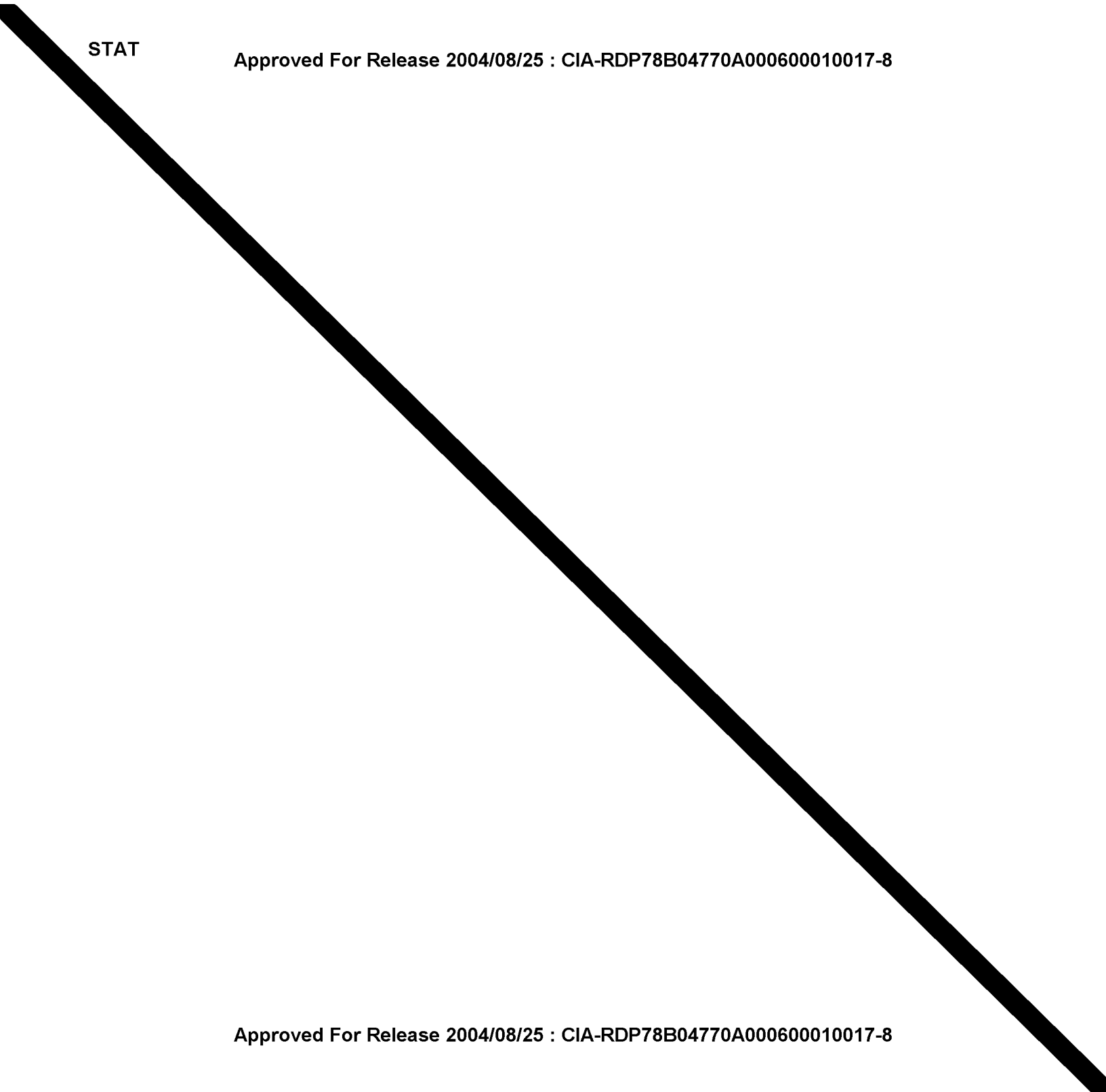

Approved For Release 2004/08/25 : CIA-RDP78B04770A000600010017-8

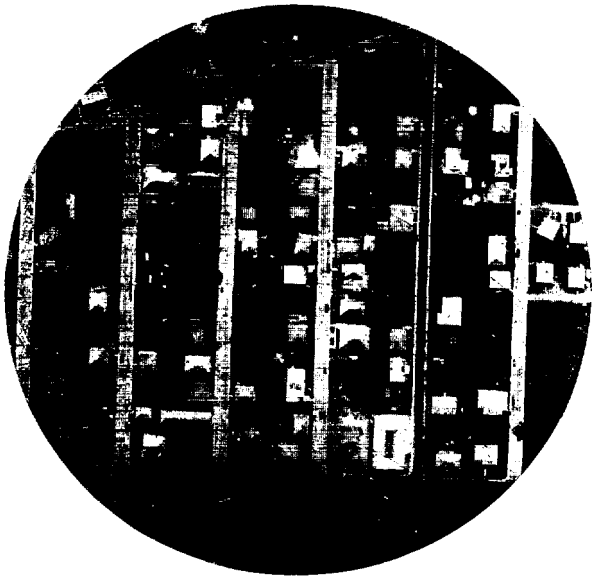

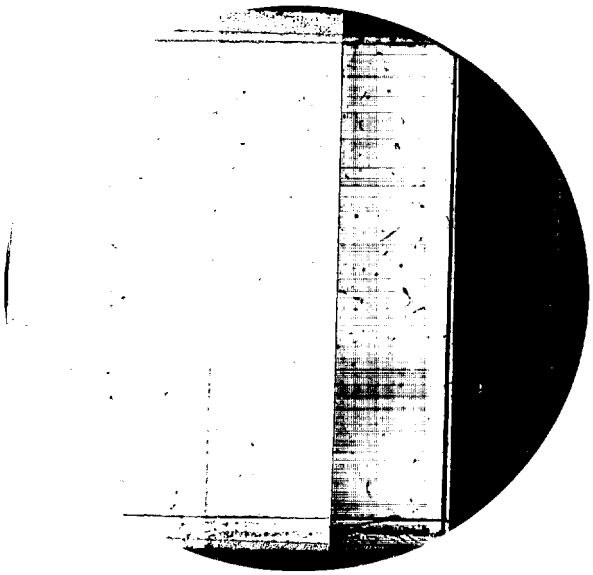

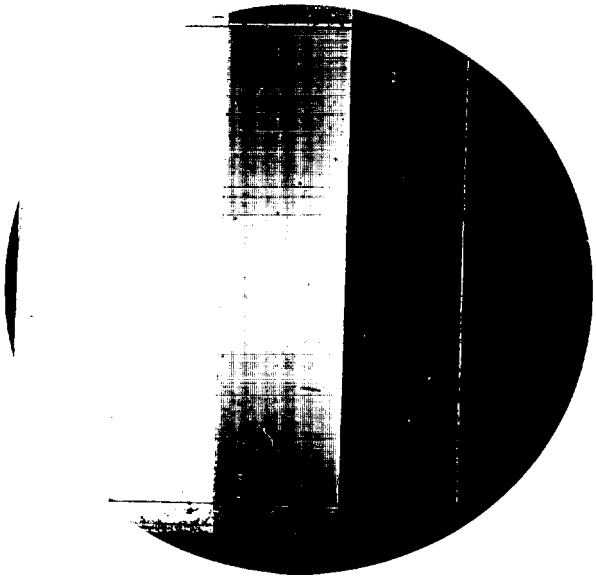

Approved For Release 2004/08/25 : CIA-RDP78B04770A000600010017-8

A. Negative Masking ≈ Perpendicular to Scanning

B. Without Negative Masking, ≈ Perpendicular to Scanning Lines

C. Negative Masking, ≈ Parallel to Scanning Lines

D. Without Negative Masking ≈ Parallel to Scanning Lines

Figure III-8. Triangular Wedges Sharp Edges, With and Without Negative Masking, ≈ Perpendicular or Parallel to Scanning Lines

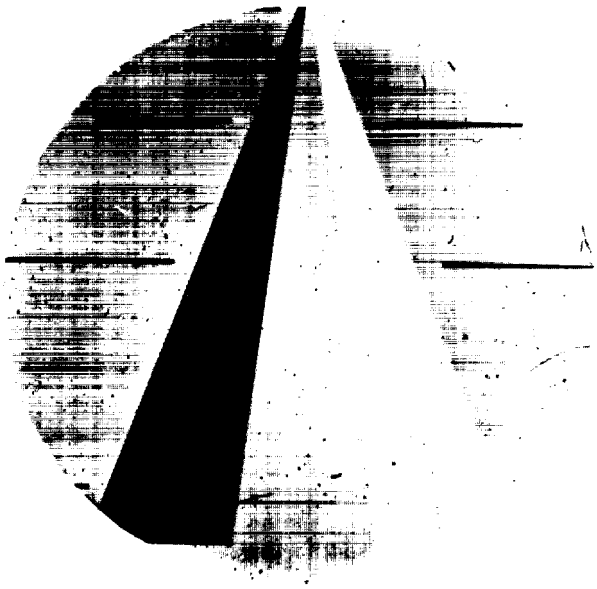

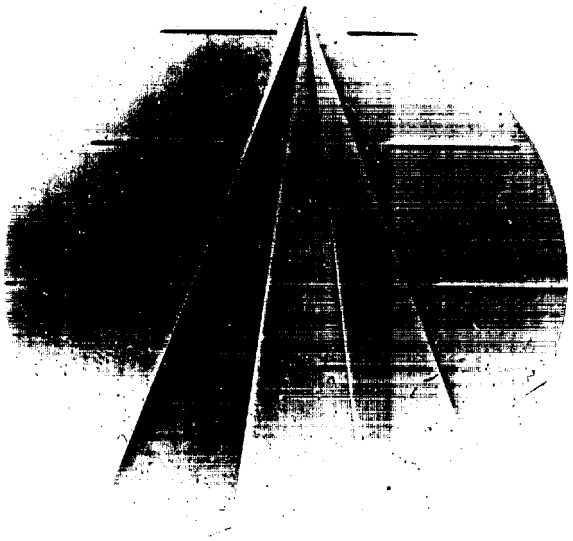

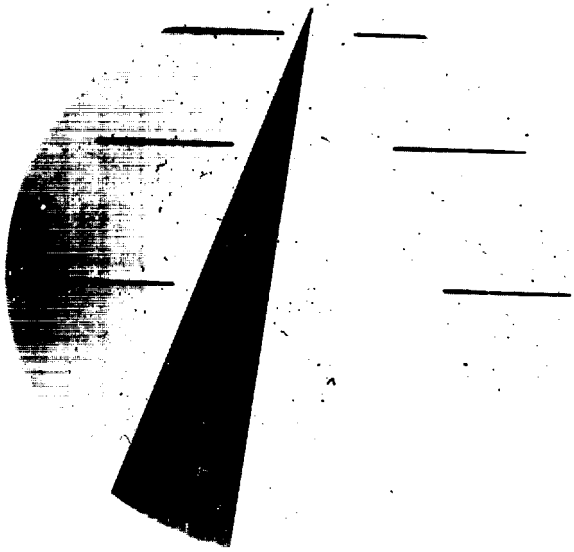

Approved For Release 2004/08/25 : CIA-RDP78B04770A000600010017-8

A. Negative Masking

B. Without Negative Masking

Effect of running the contact negative used in making View A through the system a second time.

C. Negative Masking

D. Without Negative Masking

Figure III-9. Triangular Wedges, 0.1-inch Defocussed Edges, With and Without Negative Masking ≈ Perpendicular to Scanning Lines

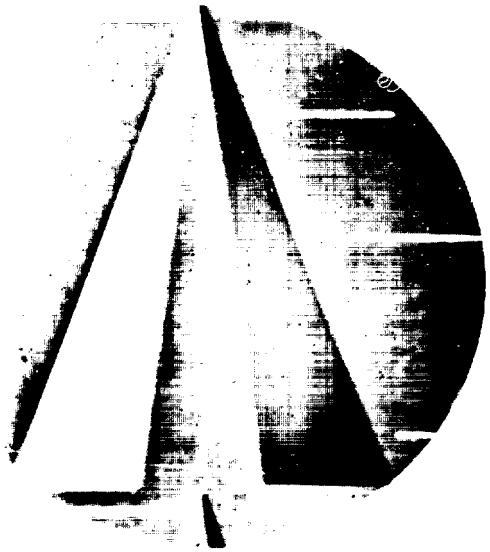

Approved For Release 2004/08/25 : CIA-RDP78B04770A000600010017-8

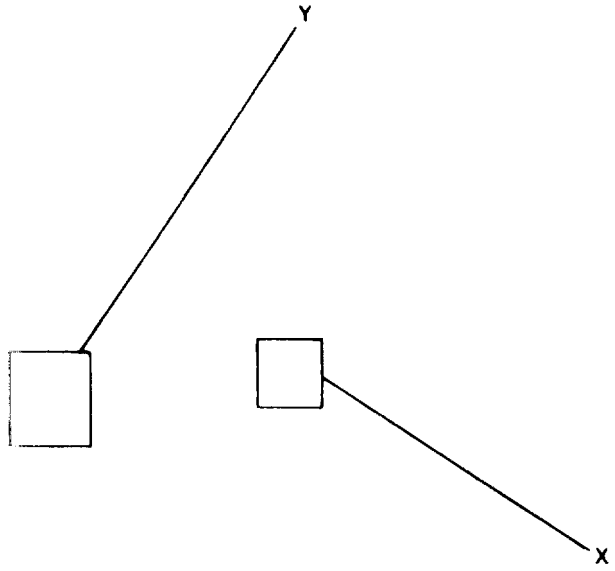


A. Negative Masking, Area X Shows Registered Dots, Area Y Shows Misregistered Dots

B. Without Negative Masking

Figure III-10. Dot Pattern With and Without Negative Masking

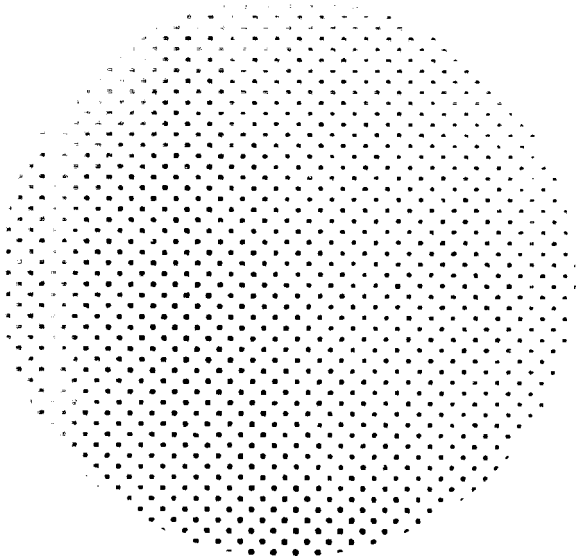

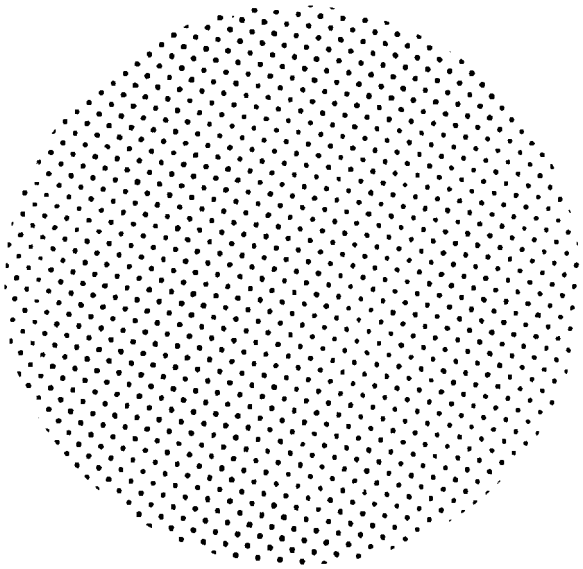

Approved For Release 2004/08/25 : CIA-RDP78B04770A000600010017-8

A. Negative Masking B. Without Negative Masking

Figure III-11. Aerial Photo of Large White Area, Trees, Buildings, etc., With and Without Negative Masking

A. Negative Masking B. Without Negative Masking

Figure III-12. Aerial Photo of Small White Areas With and Without Negative Masking

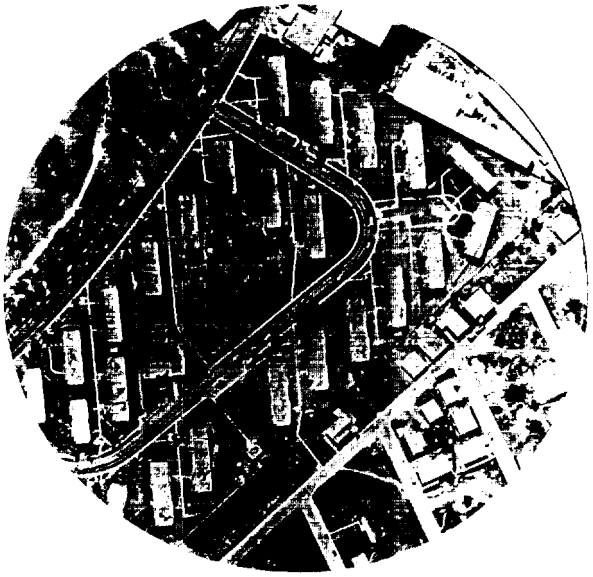

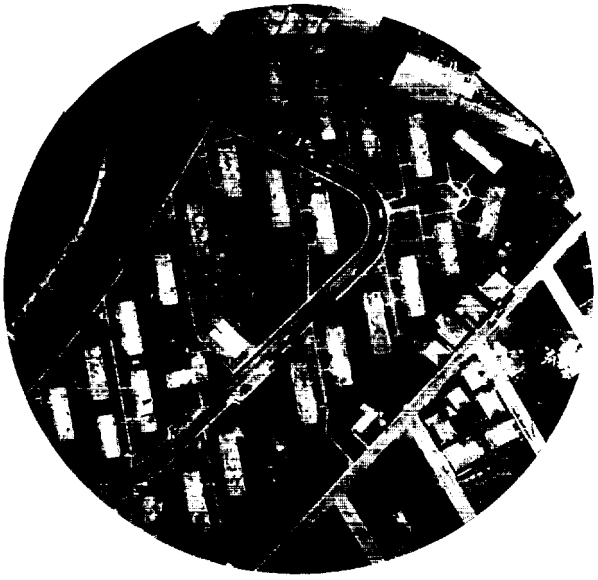

Approved For Release 2004/08/25 : CIA-RDP78B04770A000600010017-8

A. Negative Masking

B. Without Negative Masking

Figure III-13. Aerial Photo of City Streets, With and Without Negative Masking

Figure III-14. Aerial Photo with Negative Masking

Figure III-15. Aerial Photo of Mask, showing amount of mask defocussing used for all negative mask photos in this section of the report.

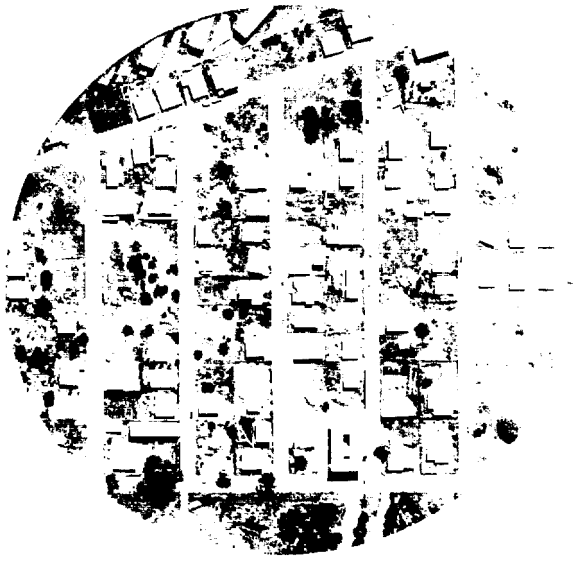

Approved For Release 2004/08/25 : CIA-RDP78B04770A000600010017-8

however, it appears that a single-kinescope system (such as [redacted] Docket No. 57520[1]) would offer several advantages over any system requiring the precise registration of several kinescopes. STAT

Work on the low-resolution breadboard has indicated the need for improvement on the high-resolution breadboard in the following areas: (1) registration, (2) shaping the video transfer characteristic, (3) resolution, and (4) increasing the video drive. These needed improvements are discussed in Paragraph C that follows.

## C. HIGH-RESOLUTION BREADBOARD

### 1. General

The high-resolution breadboard is now being assembled. It is different from the low-resolution breadboard in three important ways: (1) nine-inch Ferranti kinescopes having 0.001-inch-diameter spots are used, (2) the kinescopes and light splitters are mounted on a rigid, flat, cast-aluminum bedplate, and (3) the system deflecting capability can be operated either unidirectionally, (sawtooth scanning) or omnidirectionally, (isotropic scanning). Facilities will not be provided, however, for quickly switching from one mode to the other.

---

STAT 1. [redacted] Docket 57520 covers an open-loop feedback system that employs a single kinescope with mixed phosphors to produce modulated light for use as a contact printer. System stability is achieved by time sharing of the sensing and modulating light. System delay is compensated by delaying the video signals an amount equal to the difference between the time of one scanning line and the system delay. Vertical misregistration of one scanning line which would result from this delay is prevented by scanning each line twice: one for sensing, and once for modulation.

Lenses and light splitters are eliminated by the use of a fiber-optic faceplate on the kinescope. Although not required as a part of the modulating and printing process, a second kinescope without the fiber-optic faceplate may be used to monitor the negative light mask appearing on the modulating kinescope before and during exposure.

The main advantage of this system is that it can never get out of mechanical registry. Other advantages are better light efficiency, improved stability, and compact configuration. The main disadvantage is the high cost.

The reasons for these differences are: (1) by using kinescopes with smaller spots than previously used, the mask resolution will be improved, (2) by mounting all optical components on a rigid base, registration will be better maintained, and (3) by having different deflecting capabilities, an answer to the question as to which kind of deflection is best for a negative-mask contact printer should be satisfactorily obtained. The new deflecting components are made by [redacted] STAT to rigid specifications. They specify yokes that are electrically and mechanically identical, perpendicularity is to be held to ±0.1 percent and residual magnetism is to be held to 0.05 percent. These close tolerances should also help to improve registration over that provided by the commercial TV yokes used on the low-resolution breadboard. The resolution of the new setup will be increased from 10 to 60 cycles per millimeter, based on a 2- by 2-inch picture size; or to 120 cycles per millimeter, based on 1- by 1-inch picture size. With this flexibility, it should be possible to obtain the optimum mask resolution for a contact printer.

## 2. System Objectives

The first and probably the most important objective is to obtain contact-printed transparencies without the imperfections contributed by the low-resolution breadboard. These imperfections and the anticipated means for overcoming them have been discussed earlier in this section.

To compensate for sensing-light dilution, white stretch is required in the negative mask. This is achieved by stretching the blacks in the video transfer characteristic (remembering that white in the negative mask was originally black in the system, as shown in Figure III-16). A gamma-correcting circuit must be developed that will stretch the blacks without appreciably increasing black noise. A decrease of the system signal-to-noise ratio cannot be tolerated since the system noise is already at a marginal level. No particular difficulty is anticipated in the development of the gamma-correcting circuit. The average kinescope transfer characteristic is already stretched in the right direction; the problem presented is to enhance the existing stretch to the level desired.

If time permits, it is anticipated that those experiments that left inconclusive results on the low-resolution system will be repeated with the high-resolution system, e.g., positive edge masking, used alone or in combination with negative large-area masking.

Other uses for the high-resolution facility are connected with the evaluation of new ideas generated by examination of the electrical-chemical processing techniques study in conjunction with the electronics processing analysis model. If feasible, simulation of some of the former techniques will be considered. Likewise, the model, although primarily designed for evaluation and descriptive purposes, may suggest system modifications to be implemented and tested.

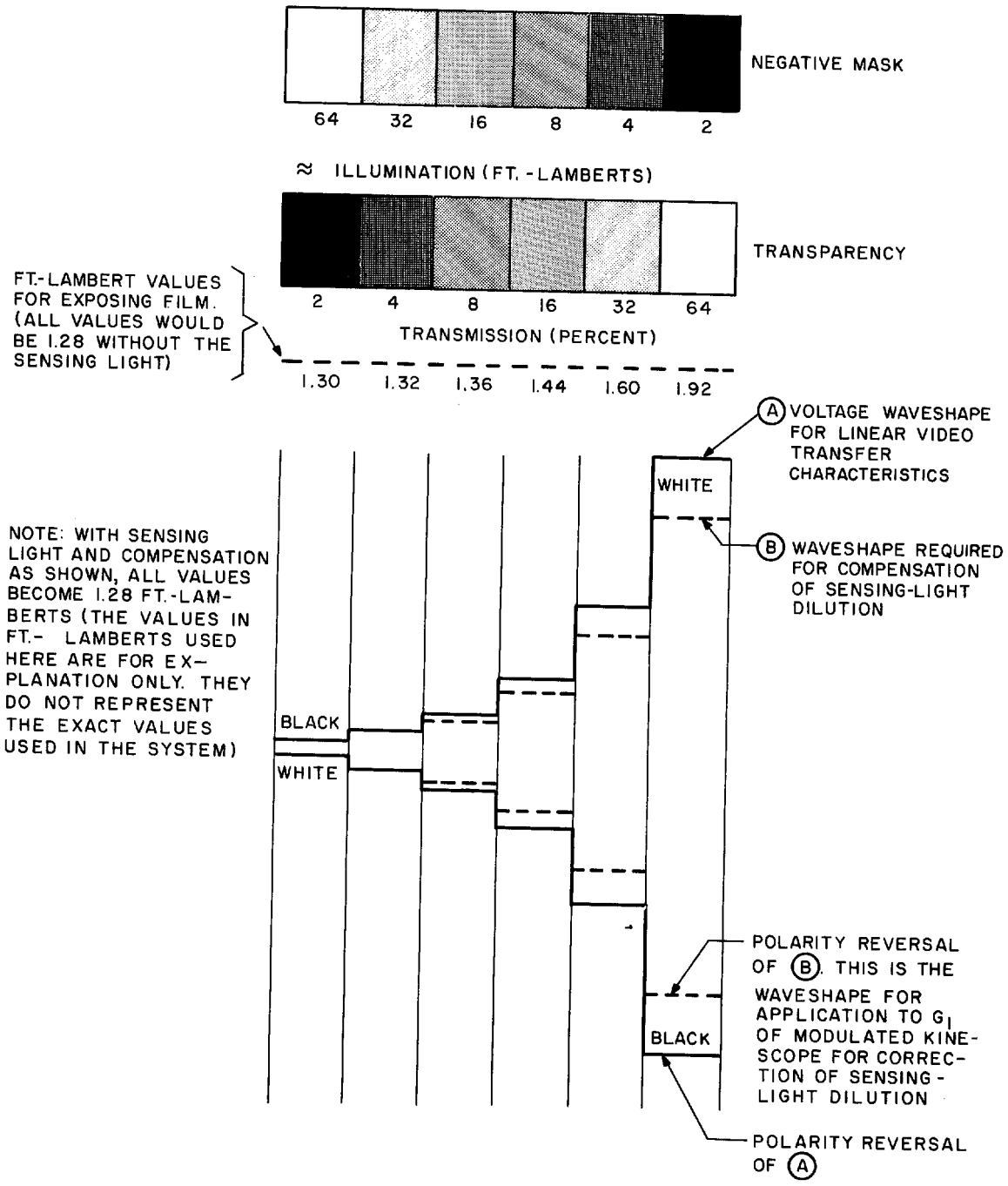


Figure III-16. Voltage Waveshape for Linear Video Transfer Characteristic and Waveshape Required for Compensation of Sensing-Light Dilution

# SECTION IV

# TECHNIQUES ANALYSIS

The objectives of the techniques analysis are to analyze and evaluate the electrical-chemical and electronic techniques employed in electrophotographic processing, to determine the performance possibilities of these techniques, and to examine the means by which they may be simulated in future all-electronic processing systems. A mathematical model of modulated-light contact-image reproducers is being developed to serve as a tool for achieving these objectives.

In the paragraphs that follow, the current status of the mathematical analysis is discussed in terms of the reproducer model, its relationship to the processing techniques, and the results obtained to date. Problem areas that have been encountered, preliminary conclusions, and plans for the next reporting period are also presented.

## A. MATHEMATICAL MODEL

A general representation of processed imagery systems is given in Figure IV-1.[2] The illustration incorporates six basic transducers: a sensor, a processor, a human, a translator, a processor controller, and a sensor controller. The system input is an object or scene; the output is a perceived image of the object. The purpose of the processor is to convert an original image of the object (i.e., the sensor output) into a processed image for display to the human interpreter. The processor employs techniques for improving image perceptibility.

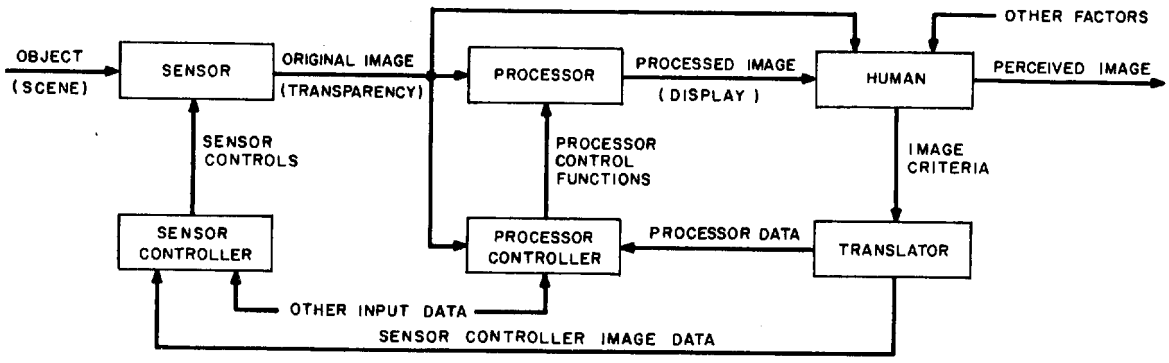


Figure IV-1. General Representation of Processed Imagery Systems

2. This Figure was given in Reference 2 and is used here for the convenience of the reader.

For the processed imagery systems of interest here, the sensor is a photographic camera whose output is recorded on a film transparency. The processor is a modulated-light contact-image reproducer: either a printer or a viewer. With respect to the general system representation, the main concern of the present study is with the processor (and processor controller). A mathematical model of modulated-light contact-image reproducers has been formulated. With the appropriate interpretation of elements and terms, the model appears to describe the operation of the breadboard cathode-ray-tube printer, the low- and high-resolution breadboard electronic processors, and the prototype film-viewing tables.

A block diagram of the modulated-light contact-image reproducer is given in Figure IV-2. This preliminary model incorporates only the major reproducer elements: the recording film, the sensing kinescope, the feedback chain (which is treated as a single element), and the modulating kinescope. Secondary elements (e.g., lenses) are not included.

The input to the reproducer, the initial image, is the photographic camera output — first recorded on a film transparency. A sensing-kinescope light beam scans the transparency to generate a light signal that is a measure of the density content of the recorded image. This light signal is then detected by a photomultiplier to yield an analogous electrical signal that can be filtered, amplified, etc. The modified electrical signal serves to drive a modulating kinescope whose light beam scans the recorded image in the identical manner of the sensing beam. Illumination of the recorded initial image with modulated-light yields an image (with respect to perceptibility), called the contact image, which can be printed or viewed directly.

For the breadboard cathode-ray-tube printer and the prototype viewing tables, both image sensing and final illuminating are performed with the same kinescope (i.e., the sensing kinescope and the modulating kinescope are embodied in the same device). For the low- and high-resolution breadboard electronic processors, there are two kinescopes and the contact image includes the effects of illuminating with the modulating kinescope and also the sensing kinescope. Finally, the feedback chain (shown as a single element in Figure IV-2) runs from the photomultiplier to the spot drive of the modulating kinescope.

## 1. Terms and Definitions

To maximize its utility, the mathematical analysis of modulated-light contact-image reproducers employs standard terms and definitions. The following applicable terms and definitions are adopted from Reference 3:

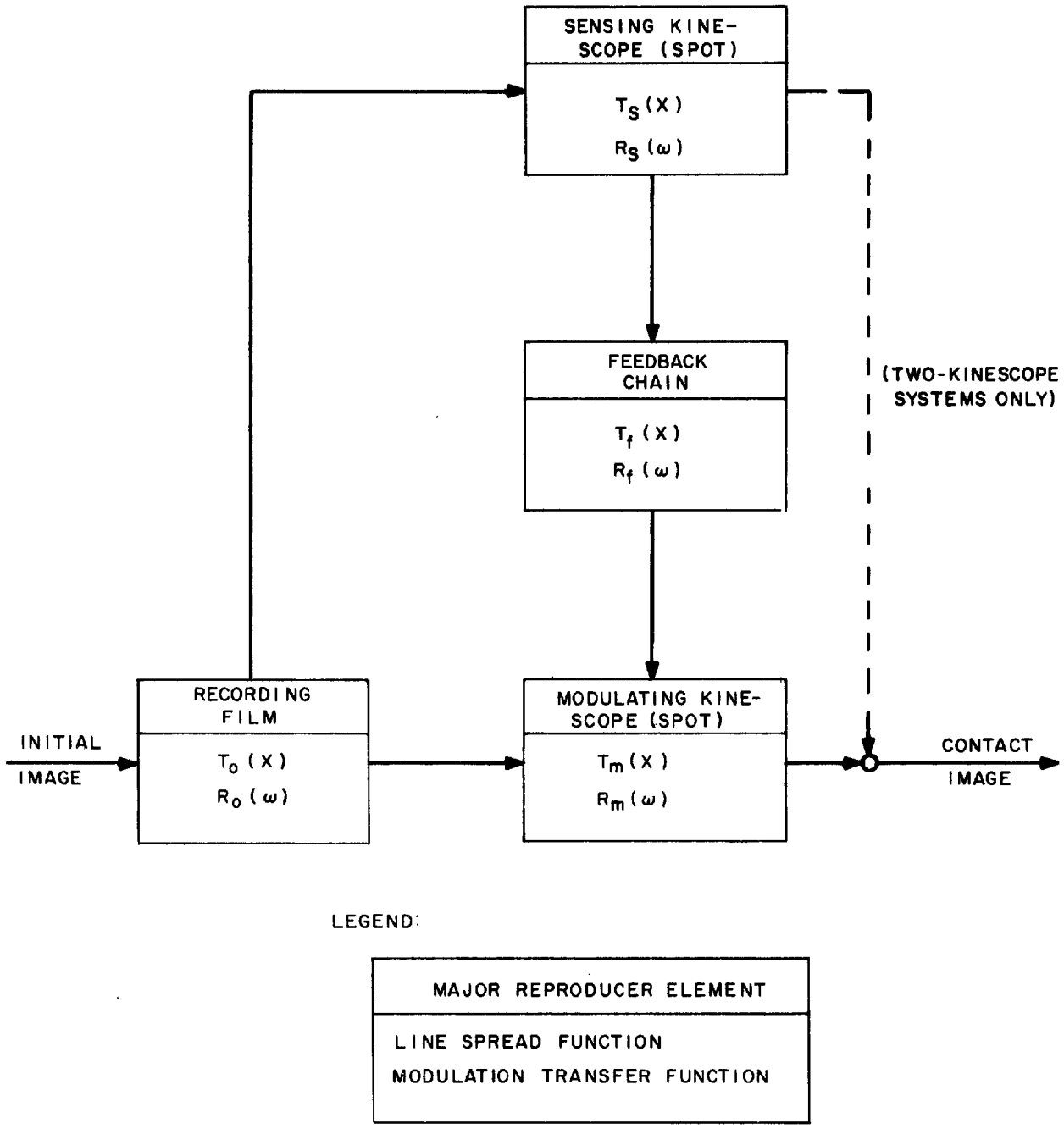


Figure IV-2. Modulated-Light Contact-Image Reproducer, Block Diagram

a. Cascaded System

A cascaded system is the tandem or series arrangements of photo-optical elements in an imagery system where the output of the preceding element directly becomes the input of the following element. Depending on the nature of the coupling between the elements, a cascaded system can in some cases be treated mathematically to give a combined function of functions of the separate elements. For example, when the output of one element goes to the next as an intensity input, then the transfer functions can be multiplied.

b. Line Spread Function (LSF)

The line-spread function is the intensity (or illuminance) distribution in the output (or image) produced by an element of a photo-optical system when the input energy corresponds to an infinitely narrow line.

c. Modulation-Transfer Function (MTF)

The modulation-transfer function is the modulus of the Fourier transform of the line-spread function. It is the ratio of the modulation at the output of a photo-optical system or element to the modulation at the input as a function of spatial frequency. (Sine-wave response, sine-wave-response function, and frequency-response function are often-used synonyms for modulation-transfer function.)

The modulated-light contact-image reproducer shown in Figure IV-2 and described above is a cascaded system that can be treated mathematically in terms of functions of its elements. Aperture theory (see, for example, References 4 and 5) shows that the elements can be described in the space domain, by line-spread functions, and in the frequency domain, by modulation-transfer functions.

d. Convolution

The convolution of one function, f(t), with a second function, g(t), is a mathematical operation that produces a third function, e(t), given by

$$e(t) = f(t) * g(t)$$

$$= \int_{-\infty}^{\infty} f(\tau)\, g(t-\tau)\, d\tau \qquad (1)$$

$$= \int_{-\infty}^{\infty} f(t-\tau)\, g(\tau)\, d\tau .$$

Convolution is thus the successive integration of the products of two functions, one "scanned" by the other. If F(w), G(w), and E(w) are the Fourier transforms of f(t), g(t), and e(t), respectively, then

$$E(w) = F(w)\,G(w). \qquad (2)$$

Hence, convolution in one domain is equivalent to multiplication in the corresponding frequency domain. (This is a well-known result of Fourier transform theory.)[3]

As an example of the above, the convolution of an object intensity distribution with a lens spread function produces the image-intensity distribution. Consider a typical reproducer element, the recording film, shown in Figure IV-3. If

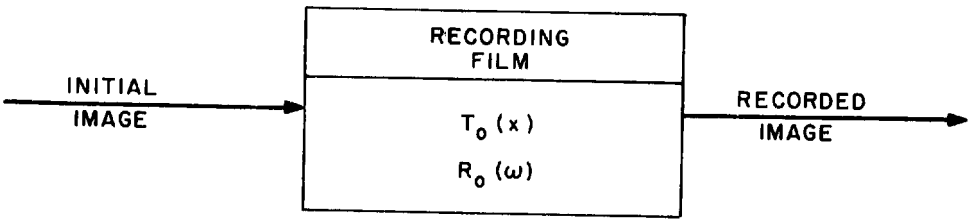


Figure IV-3. Typical Reproducer Element

$I_i(x)$ is the (linear) intensity distribution in the initial image and $T_o(x)$ is the LSF of the recording film, then the (linear) intensity distribution in the recorded image, $I_r(x)$, is

$$I_r(x) = T_o(x) * I_i(x). \qquad (3)$$

Let $S_i(\omega)$ and $S_r(\omega)$ be the moduli of the Fourier transforms of $I_i(x)$ and $I_r(x)$, repsectively, where $\omega$ is the spatial frequency corresponding to x.[4]

---

3. Strictly speaking, this discussion is applicable to linear transfer processes only.

4. As defined in Reference 3, spatial frequency is numerically the reciprocal of the distance between corresponding points on adjacent elements of a repetitive (sine-wave) pattern, and it is expressed in cycles per unit length. The "angular" spatial frequency, numerically $2\pi$ times the spatial frequency, is expressed in radians per unit length. Strict attention to the factor $2\pi$ will be paid only during the actual mathematical calculations.

Then if $R_o(\omega)$ is the MTF of the recording film,

$$S_r(\omega) = R_o(\omega)\, S_i(\omega).^{\text{(footnote 5)}} \qquad (4)$$

Similarly with Figure IV-4, if $I_i(x)$ is the (linear) intensity distribution in the initial image and $T_c(x)$ is the equivalent LSF of the cascaded system in Figure IV-2, then the (linear) intensity distribution in the contact image, $I_c(x)$, is

$$I_c(x) = T_c(x) * I_i(x). \qquad (5)$$

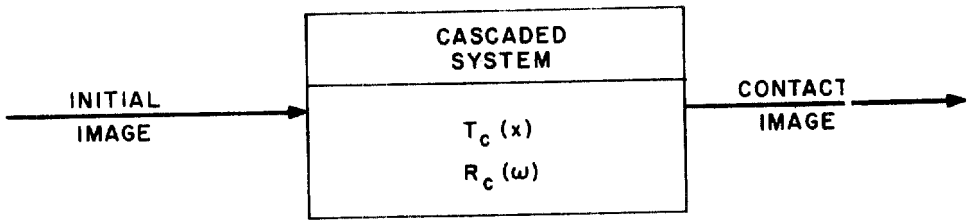


Figure IV-4. Equivalent Block Diagram

If $S_i(\omega)$ and $S_c(\omega)$ are the moduli of the Fourier transforms of $I_i(x)$ and $I_c(x)$, respectively, and $R_c(\omega)$ is the equivalent MTF of the cascaded system, then

$$S_c(\omega) = R_c(\omega)\, S_i(\omega). \qquad (6)$$

Hence, the problem of formulating a mathematical model of modulated-light contact-image reproducers is reduced to one of expressing the equivalent LSF and MTF of the cascaded system in terms of the LSF's and MTF's of the individual system elements. The derivation on the following page employs the following definitions:

| Element | LSF | MTF |
|---|---|---|
| Recording Film | $T_o(x) = T_o(0)t_o(x)$ | $R_o(\omega) = R_o(0)r_o(\omega)$ |
| Sensing Kinescope (Spot) | $T_s(x) = T_s(0)t_s(x)$ | $R_s(\omega) = R_s(0)r_s(\omega)$ |
| Feedback Chain | $T_f(x) = T_f(0)t_f(x)$ | $R_f(\omega) = R_f(0)r_f(\omega)$ |
| Modulating Kinescope (Spot)[6] | $T_m(x) = T_m(0)t_m(x)$ | $R_m(\omega) = R_m(0)\, r_m(\omega)$ |
| Cascaded System Equivalent | $T_c(x) = T_c(0)t_c(x)$ | $R_c(\omega) = R_c(0)r_c(\omega)$. |

5. The definitions of line-spread function and modulation-transfer function can be illustrated with Equations 3 and 4. If $I_i(x)$ is a unit impulse function, then $I_r(x) = T_o(x)$, the impulse response. Since the transform of a unit impulse is unity, $S_i(\omega) = 1$ and $S_r(\omega) = R_o(\omega)$, the transfer function.

6. $T_m(x)$ and $R_m(\omega)$ are actually the spread and transfer functions, respectively, of the modulating kinescope spot in the absence of modulation.

## 2. Formulation

Let the intensity distribution in the initial image be given by a unit-impulse function. Then the "output" of the recording film, the intensity distribution in the recorded image, is $T_o(x)$. The process of scanning with the sensing kinescope spot is a classic example of (aperture) convolution. Thus the "input" to the feedback chain is $T_o(x) * T_s(x)$.

The purpose of the feedback is to produce a signal for varying the intensity of the modulating kinescope spot as it scans the recorded image. (It is assumed that the normalized intensity distribution in the spot does not change with modulation.) Let $T_m(0)$ be the nominal (maximum) intensity of the modulating kinescope spot in the absence of modulation and $T_f(x)$ account for the signal transfer from the photomultiplier to the spot drive, inclusively. Then the actual intensity of the (unintegrated) spot at any point x (on the recorded image or matched kinescope raster) is $T_m(0)\left[1 - T_o(x) * T_s(x) * T_f(x)\right]$. The term $T_o(x) * T_s(x) * T_s(x)$ is actually the system's measure of the intensity transmission at the time when the sensing kinescope spot is illuminating the point x in the recorded image. Ideally, if $T_s(x)$ and $T_f(x)$ were unit impulse functions, the measure would be exactly $T_o(x)$. The system acts to produce illumination at point x that varies inversely with the measured transmission at that point. Hence the instantaneous or unintegrated kinescope spot intensity at point x is the original expression.

If the modulating kinescope possessed an ideal spot whose normalized intensity distribution was an impulse function, then the raster illumination would be exactly $T_m(0)\left[1 - T_o(x) * T_s(x) * T_f(x)\right]$. The actual intensity distribution on the modulating kinescope raster, i.e., of the integrated spots, is obtained from the convolution of this intensity function with the true normalized LSF of the kinescope spot, $t_m(x)$. If $T_m'(x)$ is the actual distribution, then

$$T_m'(x) = \left\{T_m(0)\left[1 - T_o(x) * T_s(x) * T_f(x)\right]\right\} * t_m(x). \qquad (7)$$

The process of illuminating the recorded image with the modulating kinescope raster is equivalent, in the space domain description, to multiplying the intensity distributions of the two. Hence the contribution of the modulating kinescope to the LSF of the contact image, denoted by $T_{cm}(x)$, is

$$T_{cm}(x) = T_o(x)\, T_m'(x). \qquad (8)$$

For two-kinescope systems, e.g., the low- and high-resolution breadboard electronic processors, there is also some contribution by the sensing kinescope to the LSF of the contact image. Analogous to Equations 7 and 8 are the following:

$$T'_s(x) = T_s(0) * t_s(x) \tag{9}$$

and

$$T_{cs}(x) = T_o(x)\, T'_s(x). \tag{10}$$

Equations 7 and 9 can be rewritten:

$$T'_m(x) = 1 * T_m(x) - T_o(x) * T_s(x) * T_f(x) * T_m(x \tag{7'}$$

and

$$T'_s(x) = 1 * T_s(x), \tag{9'}$$

where $1 * T_m(x)$ and $1 * T_s(x)$ serve as convenient notations for the integrated spot intensities of the modulating and sensing kinescopes, $\int_{-\infty}^{\infty} T_m(x)\, dx$ and $\int_{-\infty}^{\infty} T_s(x)\, dx$, respectively.

The equivalent LSF of the cascaded system in Figure IV-2 is given by

$$T_c(x) = T_{cm}(x) + T_{cs}(x). \tag{11}$$

Substitution of the previous expressions into Equation 11 yields a complete description of the cascaded system in the space domain:

$$T_c(x) = T_o(x)\left[1 * T_m(x) + 1 * T_s(x)\right] - T_o(x)\left[T_o(x) * T_s(x) * T_f(x) * T_m(x)\right] \tag{12}$$

By Fourier transformation, the quivalent MTF of the modulated-light contact-image reproducer can be written:

$$R_c(\omega) = R_o(\omega)\left[1 * T_m(x) + 1 * T_s(x)\right] - R_o(\omega) * \left[R_o(\omega) R_s(\omega) R_f(\omega) R_m(\omega)\right]. \tag{13}$$

The above shows that the illumination of the recorded image by the modulating kinescope raster is equivalent, in the frequency domain description, to the convolution of the transfer functions of the two. Equation 13 is a complete description of the cascaded system in the frequency domain.

### 3. Relationship to Processing Techniques

The breadboard cathode-ray-tube printer, the low- and high-resolution breadboard electronic processors, and also the prototype film-viewing tables are electronic reproducers whose major elements are completely embodied in the mathematical model. Hence Equations 12 and 13 should describe their operation — although the accuracy of the descriptions has not yet been determined.

Measurements made and phenomena observed with the low-resolution breadboard electronic processor are being studied with respect to the mathematical model. The analytical application of edge-trace measurements and the ability of the model to satisfactorily predict low-frequency suppression are discussed in Paragraph B of this section. (Measurements being made with the film viewing tables may also be reviewed in terms of the formulation.)

Electrical-chemical processing may employ techniques not yet described by the equations. The extent to which the present model can be modified to include these techniques is being investigated in parallel with their development. This analytical effort is part of the examination of the means by which useful electrophotographic techniques can be simulated in future all-electronic processing systems.

## B. ANALYTICAL RESULTS

In addition to the formulation of a mathematical model, other analytical efforts are being pursued. Results of edge-gradient investigations are discussed in the paragraphs that follow. Sample calculations performed with the model are also summarized.

### 1. Edge Gradients

The distribution of intensity or of density along the image of an edge is called an intensity edge trace or a density edge trace (see Reference 2). "Schade's "edge transition" is the intensity edge trace.

Mathematically, the derivative of the intensity edge trace is the line-spread function.[7] Hence, image edges that can be produced by straight edges in a test target or scene serve as useful and important sources for experimentally determining line-spread functions and other properties of apertures.

---

7. The intensity edge trace is obtained by scanning an image-step function with the line-spread function of the aperture. If u(x) is the image (unit) step function and T(x) is the LSF of the aperture, then the intensity edge trace is $u(x) * T(x) = \int_{-\infty}^{x} T(u)\,du$. The derivative of this function with respect to x is T(x), q.e.d.

Equations 5 and 6 show how the equivalent aperture properties of a processed imagery system can be combined with the characteristics of any initial image to yield corresponding characteristics of the processed image. In addition to analysis, system synthesis can also be performed with LSF's and MTF's. Properties of system elements can be matched to processed image requirements.

A method for obtaining the modulation-transfer function from an image edge that is especially useful for evaluating images not containing test targets, is described in Reference 6. Microdensitometric data (i.e., a density edge trace) is treated to yield the square-wave response from which the sine-wave response or modulation-transfer function is determined.

To illustrate this discussion of aperture properties, a simple modulated-light image processor is defined as a cascaded system in which an unsharp negative mask is optically added to a given image. Such a system might look like that shown in Figure IV-5, where the raster of the modulating kinescope displays the mask. The expected equivalent aperture properties of the simple system are shown in Figure IV-6.

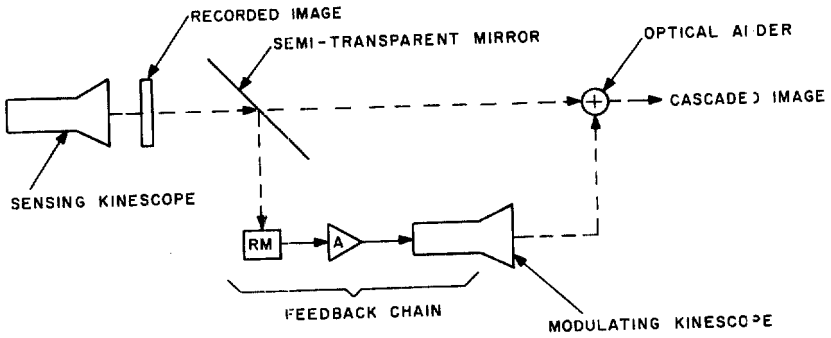


Figure IV-5. Representation of Simple Modulated-Light Image Processor

It should be noted that the contact-image reproducer is not a simple processor (as defined) because with it, the modulated illumination passes through the recorded image. This light, therefore, multiplies the image signal rather than adds to it as is the case for the simple processor. The contact-image reproducer affords information transfer, with higher fidelity. The simple processor, however, can serve as a standard for understanding the more-complex contact-image reproducer.

Two basic phenomena associated with the simple processor are readily observed in Figure IV-6: space-domain overshoot, i.e., the enhancement of edges due to blacks going blacker than "black" and whites going whiter than "white", and low-frequency suppression. These phenomena are also exhibited by modulated-light contact-image reproducers.

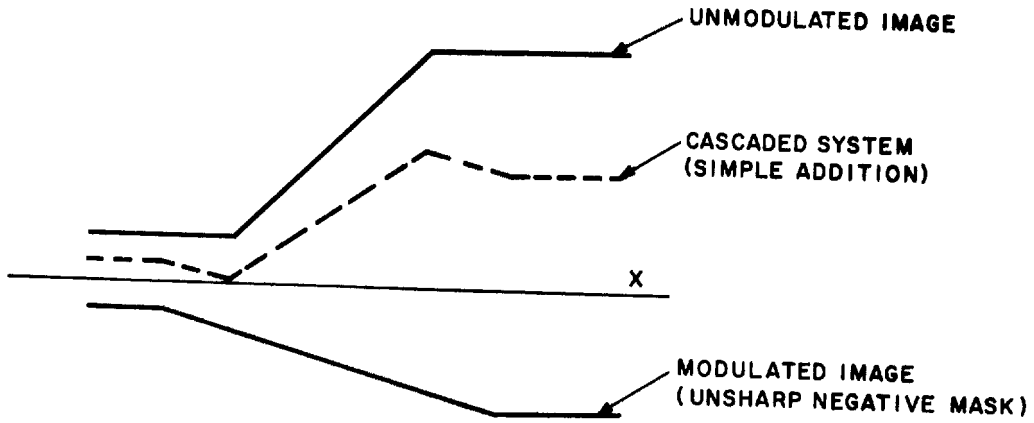


A. INTENSITY EDGE TRACES

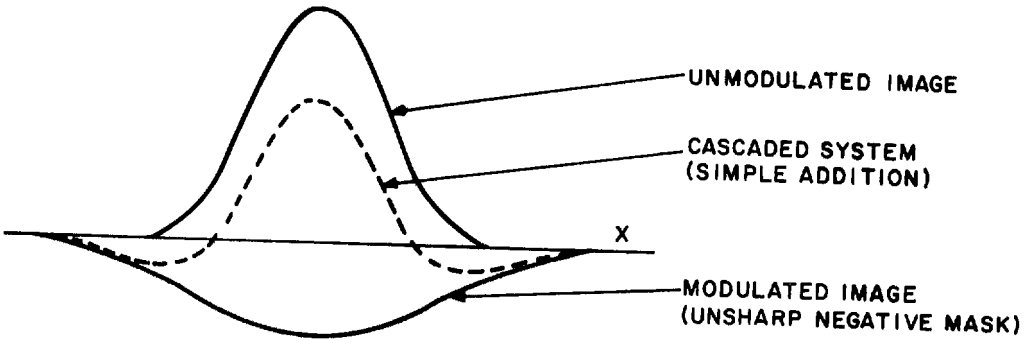


B. LINE SPREAD FUNCTIONS

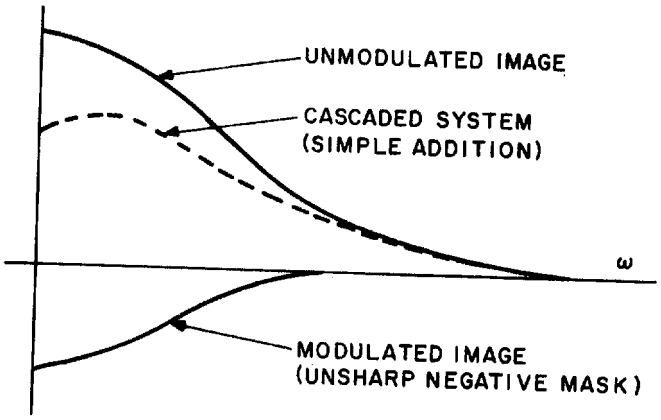


C. MODULATION TRANSFER FUNCTIONS

Figure IV-6. Equivalent Aperture Properties of Simple Image Processor

Consideration of the simple modulated-light image processor has aided the analysis of the more complex (mathematically, at least) contact-image reproducer. For example, density edge traces have been obtained experimentally with the low-resolution breadboard electronic processor. The tests employed the focussed and unfocussed triagnle test targets shown in Section II. All the edge traces displayed the previously cited space domain overshoot to some extent.

The analysis of these density edge traces is proceeding along the lines discussed above. However, two additional points should be noted. The width of each trace normally reflects the width of the microdensitometer slit. Also, the effective width of the slit is increased because the image edge is not perpendicular to the direction of scan by the slit. The analysis, therefore, includes compensation for these effects.

## 2. Sample Calculations

As part of the continuing development of the mathematical model of the modulated-light contact-image processor, sample calculations have been performed with Equations 12 and 13. An example is given below.

For the present purpose, Equation 12 is written in terms of the normalized LSF's of the system elements.

$$T_c(x) = K_1 t_o(x) - K_2 t_o(x) \left[ t_o(x) * t_s(x) * t_f(x) * t_m(x \right] \qquad (12')$$

Assume, for simplicity, that both kinescope spots have identical Gaussian LSF's given by $t_s(x) = t_m(x) = \exp(-bx^2)$ and that the feedback chain LSF is an impulse function.

Next, assume that the LSF of the recording transparency is given by $t_o(x) = A_1 f(x, x_o) + A_2 \exp(-ax^2)$, where $A_1$ and $A_2$ are functions of the contrast in the recorded image ($A_1 + A_2 = 1$) and $f(x, x_o)$ accounts for the finite width ($2x_o$) of the transparency. If $u(x)$ is the unit step function, then $f(x, x_o) = u(x) - u(x - x_o)$. The function $t_o(x)$ is Gaussian in nature.

With these assumptions and the Schade rule for convolving normalized LSF's: the convolution of two normalized LSF's produces a third <u>normalized</u> LSF, it can be shown that

$$t_o(x) * t_s(x) * t_f(x) * t_m(x) = A_1 g(x, x_o) + A_2 e^{-\frac{a(b/2)}{a+b/2} x^2}, \qquad (14)$$

where

$$g(x, x_o) = \frac{\operatorname{erf}\left[(x_o - x)\sqrt{b/2}\right] + \operatorname{erf}\left[(x_o + x)\sqrt{b/2}\right]}{2\operatorname{erf}\left[x_o \sqrt{b/2}\right]}.$$

Fortunately, for b's corresponding to beam resolutions of the order of 100 cycles per millimeter and film (transparency) widths of the order of 10 inches, $g(x, x_o)$ is very nearly unity in the range $-x_o \leq x \leq x_o$.

Hence, from Equation 12′,

$$T_c(x) = \left[A_1 f(x, x_o) + A_2 e^{-ax^2}\right] \cdot \left[K_1 - K_2 \left\{A_1 g(x, x_o) + A_2 e^{-\frac{a(b/2)}{a+b/2} x^2}\right\}\right]$$

$$\approx \left[A_1 f(x, x_o) + A_2 e^{-ax^2}\right] \left[K_1 - K_2 \left\{A_1 + A_2 e^{-\frac{a(b/2)}{a+b/2} x^2}\right\}\right] \qquad (15)$$

in the range of interest. Equation 15 is depicted in Figure IV-7. Note the strong similarity between the cascaded system LSF's in Figure IV-7 and Figure IV-6(B).

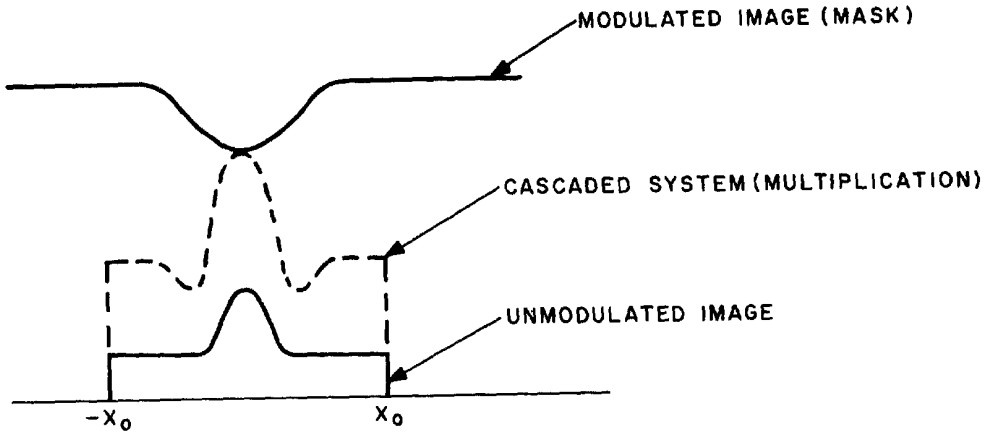


Figure IV-7. Equivalent Line-Spread Function of Contact-Image Processor

With the simple processor, space-domain overshoot results directly from the addition of the unsharp negative mask. With the contact-image reproducer, it results from the multiplication of the unsharp negative mask. Both systems procude enhanced edges.

For the present purpose, Equation 13 is written in terms of the normalized MTF's of the system elements:

$$R_c(\omega) = C_1 r_o(\omega) - C_2 r_o(\omega) * r_o(\omega)\, r_s(\omega)\, r_f(\omega)\, r_m(\omega). \qquad (13')$$

From the above assumptions, $r_s(\omega) = r_m(\omega) = \exp(-\omega^2/4b)$, $r_f(\omega) = 1$, and $r_o(\omega) = A_1(\sin \omega x_o)/\omega x_o + A_2 \exp(-\omega^2/4a)$. With these expressions and the rule for convolving normalized functions, it can be shown (assuming b and $x_o$ are of the same orders of magnitude as before) that

$$R_c(\omega) \approx C_3 \left[ A_1 \frac{\sin \omega x_o}{\omega x_o} + A_2 e^{-\frac{\omega^2}{4a}} \right] - C_4 A_1 e^{-\frac{\omega^2}{\frac{4a(b/2)}{a+b/2}}} - C_4 A_2 e^{-4a \frac{\omega^2}{a+b/2}}, \qquad (16)$$

where $C_3 = C_1 - C_2 A_1$ and $C_4 = C_2 A_2$.

Equation 16 is not easily illustrated. However, the expression is being analyzed mathematically, especially with respect to its low-frequency properties.

## C. PRELIMINARY CONCLUSIONS AND PLANS

Some preliminary conclusions of the techniques analysis to date are discussed below. Plans for work on this task in the next reporting period (which will be covered in the Final Report) are also presented.

A mathematical model of modulated-light contact-image reproducers has been formulated. With the appropriate interpretation of elements and terms, the model appears to describe the operation of the breadboard cathode-ray-tube printer, the low- and high-resolution breadboard electronic processors, and also the prototype film-viewing tables. The extent to which the model can be modified to include other electrophotographic techniques has not yet been determined.

The model shows that contact-image reproducers differ from the previously defined simple modulated-light processors exhibiting unsharp negative masking. But consideration of the simple processor has aided the understanding of the more-complex system. Equations derived from the model have already illustrated the effect called space-domain overshoot. As yet, however, they have not satisfactorily demonstrated low-frequency suppression.

The mathematical model is a most useful tool for analyzing and evaluating techniques employed in electrophotographic processing, for determining the performance limitations of these techniques, and for examining the means by which they may be simulated in future all-electronic processing systems. However, the need for further development of the model is indicated.

The density (or intensity) edge trace provides the means for experimentally determining the equivalent aperture properties of modulated-light contact-image reproducers. Edge-gradient measurements can be incorporated directly into calculations based upon the mathematical model. However, care must be taken when interpreting the experimental results.

The calculated LSF's and MTF's will provide calibration-like measurements of the systems and their elements. These functions will reflect design changes and also serve to direct system modifications. For example, after stating his requirements in terms of the LSF's and MTF's, the systems synthesizer can use these as bases for his designs. (By knowing the "output" characteristics and those of some of the elements, he can derive the requirements for the variable elements.)

Based upon these conclusions and others indicated by the discussions above, the following work is planned for the next reporting period:

1. Completion of the "checkout tests" of the mathematical model (i.e., complete the mathematical analysis of Equation 16).
2. Completion of the mathematical analysis of the density edge traces obtained with the low-resolution breadboard electronic processor utilizing, for the most part, the method of derivatives for obtaining the LSF and the method described in Reference 6 for obtaining the MTF associated with each edge trace.
3. Analyze density edge traces to be obtained with the breadboard cathode-ray-tube printer and high-resolution breadboard electronic processor.
4. Analyze density edge traces to be obtained with overall electrical-chemical processing.
5. Incorporate the density edge trace measurements into the equations derived from the mathematical model.
6. Modify the model as required.
7. Use the model and all other appropriate tools to determine the performance capabilities of the various electrophotographic processing techniques employed in the program.
8. Use the model and all other appropriate tools to examine and suggest the means by which the promising techniques may be simulated in future all-electronic processing systems.
9. Utilize, to the extent possible, the results of other related programs.
10. Recommend additional experimental and analytical efforts, not within the scope of the present program, for consideration by the Government.

## REFERENCES

1. Encyclopedia of Microscopy.

STAT [redacted]

4. O.H. Schade, SMPTE Series, "Image Gradation, Graininess and Sharpness in Television and Motion-Picture Systems":
Part I: "Image Structure and Transfer Characteristics," Jour. SMPTE, Vol. 56, No. 2 (February 1951).
Part II: "The Grain Structure of Motion-Picture Images—An Analysis of Deviations and Fluctuations of the Sample Numbers, "Jour. SMPTE, Vol. 58, No. 3 (March 1952).
Part III: "The Grain Structure of Television Images," Jour. SMPTE, Vol. 61, No. 2 (August 1953).
Part IV: "Image Analysis in Photographic and Television Systems (Definition and Sharpness)," Jour. SMPTE, Vo. 64, No. 11 (November 1955).

5. O.H. Schade, "An Evaluation of Photographic Image Quality and Resolving Power," Jour. SMPTE, Vol. 73, No. 2 (February 1964).

6. F. Scott, R.M. Scott, and R.V. Shack, "The Use of Edge Gradients in Determining Modulation-Transfer Functions," Photo. S&E, Vol. 7, No. 6 (November-December 1963).